Further characterisation of late somatosensory evoked potentials using EEG and MEG source imaging

Sahar Hssain-Khalladi, Alain Giron, Clément Huneau, Christophe Gitton,
Denis Schwartz, Nathalie George, Michel Le van Quyen, Guillaume Marrelec,
Veronique Marchand-Pauvert

Further characterisation of late somatosensory evoked potentials using EEG and MEG source imaging

Running title: Cortical origin of late SEPs

Sahar Hssain-Khalladi[1,2], Alain Giron[1], Clément Huneau[3], Christophe Gitton[4], Denis Schwartz[4], Nathalie George[4], Michel Le Van Quyen[1], Guillaume Marrelec[1*], Véronique Marchand-Pauvert[1*]

*G. Marrelec and V. Marchand-Pauvert are co-last authors

1. Sorbonne Université, Inserm, CNRS, Laboratoire d'Imagerie Biomédicale, LIB, F-75006, Paris, France
2. Sorbonne Université, Laboratoire d'Excellence SMART, F-75005, Paris, France
3. Université de Nantes, CNRS, Laboratoire des Sciences du Numérique de Nantes, LS2N, Nantes, France
4. Sorbonne Université, Inserm, CNRS, Institut du Cerveau, ICM, F-75013, Paris, France

Correspondance to:

Véronique Marchand-Pauvert

veronique.marchand-pauvert@inserm.fr

Laboratoire d'Imagerie Biomédicale (LIB) - Campus des Cordeliers – Bât. A, 3e étage

15 rue de l'Ecole de Médecine - 75006 Paris, France

ABSTRACT

Beside the well documented involvement of secondary somatosensory area, the cortical network underlying late somatosensory evoked potentials (P60/N60, P100/N100) is still unknown. Electro- and magnetoencephalogram source imaging were performed to further investigate the origin of the brain cortical areas involved in late somatosensory evoked potentials, using sensory inputs of different strengths, and by testing the correlation between cortical sources. Simultaneous high-density electro- and magnetoencephalograms were performed in 19 participants, and electrical stimulation was applied to the median nerve (wrist level) at intensity between 1.5 and 9 x the perceptual threshold. Source imaging was undertaken to map the stimulus-induced brain cortical activity according to each individual brain magnetic resonance imaging, during 3 windows of analysis covering early and late SEPs. Results for P60/N60 and P100/N100 were compared to those for P20/N20 (early response). According to literature, maximal activity during P20/N20 was found in central sulcus contralateral to stimulation site. During P60/N60 and P100/N100, activity was observed in contralateral primary sensorimotor area, secondary somatosensory area (on both hemispheres), premotor and multisensory associative cortices. Late responses exhibited similar characteristics, but different from P20/N20, and no significant correlation was found between early and late generated activities. Specific clusters of cortical activities were activated with specific input/output relationships underlying early and late SEPs. Cortical networks, partly common to and distinct from early somatosensory responses contribute to late responses, all participating in the complex somatosensory brain processing.

Keywords: Somatosensory evoked potentials, EEG, MEG, Source Imaging, Brain mapping, Humans

Abbreviation list:

ECG, electrocardiogram; **EEG**, electroencephalogram; **EOG**, electrooculogram; **I/O**, input-output ratio; **iPPC**, inferior posterior parietal cortex; **ISI**, interstimulus interval; **M1**, primary motor cortex; **MEG**, magnetoencephalogram; **MRI**, magnetic resonance imaging; **MT**, motor threshold; **PCC**, posterior cingulate cortex; **PM**, premotor cortex; **PT**, perceptual threshold; ; **ROI**, regions of interest; **SEP**, somatosensory evoked potentials; **SI**, primary somatosensory area; **SII**, secondary somatosensory area; **SMA**, supplemental motor area; **SMG**, supramarginal area; **sPPC**, superior posterior parietal cortex; **STS**, superior temporal sulcus.

INTRODUCTION

Somatosensory evoked potentials (SEPs) are investigated in clinics to evaluate the integrity of the peripheral and central sensory pathways. In clinical routine, sensory inputs are produced by stimulating peripheral nerves electrically, and the resulting cortical responses are most often collected with small single-use needles inserted in the scalp, at the C3/C4 standard electroencephalogram (EEG) locations *i.e.*, over the primary sensorimotor cortex, contralateral and ipsilateral to the stimulation site. The reference electrode is extra-cephalic, most often using a pre-gelled surface electrode stuck on one ear lobe. The signals from the contralateral and ipsilateral cortices are then subtracted from each other, to evaluate the amplitude of the first biphasic response *i.e.*, N20-P25 component (Morizot-Koutlidis *et al.*, 2015). In line with the clinical use of SEPs, most of the researches focused on the early components of cortical SEPs, with latency < 35 ms (Passmore *et al.*, 2014); the late components (> 35 ms) have been investigated to a much lesser extent. In a previous study, we reported that the late SEPs (P60/N60 and P100/N100) are more depressed in patients with amyotrophic lateral sclerosis (ALS), compared to earlier components (P20/N20, P25/N25 and P30/N30), and we did not find any correlation between the early and late components (Sangari *et al.*, 2016). Despite existing literature, questions remain on the precise origin and characteristics of late components (source locations and sensitivity to peripheral inputs) and interaction with earlier components, to evaluate the altered cortical excitability in patients with ALS.

Based on dipole localisation from scalp, epidural and intracranial EEG, it has been well established that P20/N20 is generated in the primary somatosensory area (SI), and that the following peaks, P25/N25 and P30/N30, are likely due to activity in posterior parietal, motor and premotor areas (Allison *et al.*, 1991; Mauguiere, 2005; Passmore *et al.*, 2014). Much less is known on later components with latency > 40 ms, but it has been admitted that the secondary somatosensory cortex (SII) might be particularly involved in P60/N60 and P100/N100, and to a lesser extent in earlier responses with latency < 40 ms (Allison *et al.*, 1991; Mauguiere, 2005; Passmore *et al.*, 2014). Several methods of source imaging, based on the resolution of inverse problem, have been developed using

81 magnetoencephalography (MEG) and EEG (see for references Baillet, 2017; Michel & He, 2019). Their

82 first applications to SEPs gave rise to consistent results with previous studies using dipole

83 localisation, regarding the origin of P20/N20 in SI, and the area 3b in particular (Allison *et al.*, 1991;

84 Buchner *et al.*, 1994; Nakamura *et al.*, 1998). Later, P20/N20 was used to develop new methods of

85 source imaging, to compare their abilities to localise the dipole in SI and to test the influence of

86 stimulation type, head modelling and the use of combined or separate MEG/EEG recordings (Komssi

87 *et al.*, 2004; Huang *et al.*, 2007; Mideksa *et al.*, 2012; Antonakakis *et al.*, 2019; Rezaei *et al.*, 2021).

88 However, to date, the cortical activation map after peripheral nerve stimulation and its temporality

89 has not been studied in detail. Specifically, there is no detailed report of source location (except SII)

90 during late components while this would help to deepen the knowledge on the origin of the late

91 cortical responses to peripheral nerve stimulation (cortical map of induced activity, interaction

92 between early and late components and between cortical areas involved).

93   Previous studies have explored the influence of stimulation intensity on the early and late

94 components and on the responses of SI or SII areas, assuming that if the input/output (I/O)

95 relationships are different between early and late components, or between SI and SII cortical areas,

96 the underlying neural encoding is different and likely plays a different role in the somatosensory

97 brain processing (Huttunen, 1995; Jousmäki & Forss, 1998; Gerber & Meinck, 2000; Torquati *et al.*,

98 2002; Lin *et al.*, 2003; Onishi *et al.*, 2013). Globally, all these studies revealed that the somatosensory

99 evoked cortical responses increased with sensory afferent inputs. Regarding the intensity of electrical

100 stimulus, the size of the dipoles increased with stimulus strength before they plateaued at intensity

101 around the motor threshold (1 x MT; threshold intensity for activating the motor axons in the

102 peripheral nerve). There was a trend that the increase was more marked for the early components

103 and SI responses, while the changes in the late components and SII responses were more

104 heterogenous, especially at intensities > 1 x MT. These results support the commonly accepted link

105 between early SEP components and SI on one hand, and the one between late components and SII

106 on the other hand. However, none of these studies has combined EEG and MEG, or has investigated

107   the influence of the intensity of peripheral nerve stimulation on source activities in all brain cortex.

108   Lastly, the intensity of peripheral nerve stimulation was not normalised or normalised using different

109   methodologies (relative to MT or to the perceptual threshold [PT] or mixing both) while according to

110   experimental setup and conditions, raw intensity (in mA) are not comparable from one subject to

111   another and from one study to another. Furthermore, it has been shown that normalising the

112   stimulus intensity to PT gave more consistent results regarding the size of SEPs (Fukuda *et al.*, 2007)

113   but this procedure has not been standardized across studies yet.

114   Consequently, the present study was designed to further investigate the origin and the

115   characteristics of the late components, P60/N60 and P100/N100, in healthy conditions. Indeed,

116   detailed examination of the late components would be an added value for the evaluation of the

117   somatosensory integrations at higher processing level, involving extra sensorimotor cortical areas

118   involved in cognitive processes (*e.g.*, motor learning) and executive functions (*e.g.*, motor planning).

119   To this end, SEPs were produced by median nerve electrical stimulations delivered at the wrist level

120   in neurologically intact participants. The stimulus intensity was normalised to PT and varied between

121   1.5 and 9 x PT *i.e.*, below and above MT (being between 3 and 6 x PT according to our experience).

122   EEG and MEG responses were recorded simultaneously and the time series were analysed within the

123   time windows covering the first component P20/N20 and the late ones, P60/N60 and P100/N100.

124   Source imaging for the 3 components was performed to identify the brain regions significantly

125   activated by median nerve stimuli. Based on the localisation of MEG sources at the group level (given

126   its greater spatial accuracy compared to EEG; Leahy *et al.*, 1998; Komssi *et al.*, 2004; Baillet, 2017),

127   we determined the regions of interest (ROIs) to compare the source activities according to the

128   stimulus intensity. Statistical analyses were undertaken to compare the characteristics (source

129   location, relationship with stimulus intensity) of early and late responses, their possible links and the

130   interaction between cortical areas (ROIs) involved in these responses.

131

MATERIALS & METHODS

Ethical statement

The study was conducted in accordance with the latest revision of the Declaration of Helsinki. The procedures were approved by the CNRS ethic committee (study #1402) and by the national ethical authorities (CPP Ile de France, Paris 6 – Pitié-Salpêtrière and ANSM; IRB 2015-A00462-47). All subjects provided their written informed consent prior to their inclusion in the research protocol. The data that support the findings of this study are available on request from NG among the authors; they are not publicly available due to ethical restrictions.

Participants

The inclusion criteria were: i) no drug intake affecting the neural excitability (psychotropic drugs), ii) no history of stroke, head trauma, heart disease, peripheral neuropathy, or diabetes, and iii) no metal implant or pacemaker. Twenty-two (22) healthy subjects were included in the protocol. EEG and MEG recordings could not be performed in 1 of them due to ferromagnetic incompatibility (dental implants) and, in 2 others, the anatomical magnetic resonance imaging (MRI) could not be segmented properly because of motion artefact. Accordingly, the dataset in the present study included 19 subjects: 13 females, 18 right-handed participants (Oldfield, 1971), with age ranging between 22 and 61 years old (mean ± standard error, [SE]: 32.5 ± 2.6 years old). The experiments were performed at the Centre of Neuroimaging Research (CENIR)-EEG/MEG Centre of the Brain Institute (ICM, Pitié-Salpêtrière Hospital, Paris, France).

Simultaneous EEG/MEG

Elekta® Neuromag (TRIUX, Stockholm, Sweden) allowing synchronous EEG and MEG recordings was used. EEG cap with 74 Ag/AgCl annular electrodes was placed according to the international 10/20 system (EasyCap GmbH, Herrsching, Germany; Nuwer 2018). It was positioned so that the Cz electrode was over the anatomical vertex point in each volunteer. Water soluble conducting-gel was injected in each electrode and impedance was checked individually (~5-10 kΩ) before acquisition. Single-use pre-gelled Ag/AgCl electrodes (Ambu® Neuroline 720, Ballerup, Denmark) were placed

158   over the right ear lobe for the reference electrode and on the left scapula for the ground electrode.

159   MEG included 306 superconducting quantum interference devices (SQUIDs) with 102 radial

160   magnetometers and 204 axial gradiometers on the scalp.

161   Anatomical landmarks were captured including nasion, left and right pre-auricular points (LPA

162   and RPA, respectively) and up to 70 points over the scalp with a 3-dimensional scanning system

163   (Polhemus 3D Fastrak, Colchester, VT, USA) to digitalise the head shape of each volunteer. EEG

164   electrode location was also recorded. Two head position indicator (HPI) coils were placed on the

165   superior part of the forehead, on the right and the left sides, and 2 other ones, on the right and left

166   mastoids. Before each recording session, a weak alternating current was injected in the HPI coils

167   (electrically isolated from the subject), to generate a magnetic field captured by MEG sensors. This

168   field was used to detect the position of HPI coils in the MEG helmet and to ensure that head position

169   did not change between each acquisition. All the procedure (head shape digitalisation, location of

170   EEG electrodes and HPI coils) allowed to reconstruct the head position in the MEG-EEG devices.

171   The electrooculogram (EO') and the electrocardiogram (EC') were recorded simultaneously, to

172   get a continuous recording of non-cerebral electrophysiological activities. These recordings were

173   performed using single-use pre-gelled electrodes (same type of electrodes as the reference and

174   ground electrodes) placed above and below the right eye and on the right and left temples for EOG,

175   and on the right clavicle and the left part of lower abdomen for ECG.

176   The amplifiers and the entire electronic part of the EEG system (also collecting EOG and ECG)

177   were integrated into the MEG system, using the same internal clock to synchronise all acquisitions.

178   Therefore, all signals (EEG, MEG, EOG and ECG) were collected simultaneously. All signals were

179   filtered (1000-Hz lowpass filter for all, 0.03-Hz high-pass for EEG and 0.1-Hz high-pass for EOG and

180   ECG) and digitalised using 3-kHz sampling rate.

181   **Experimental procedure**

182   After the subjects were prepared for EEG, EOG and ECG recordings outside the shielded MEG

183   room, they were comfortably installed in the MEG chair whose position was adjusted so as the top of

184   their head touched the top of the MEG helmet. All the electrodes for EEG, EOG, ECG and the HPI coils

185   were connected to the EEG-MEG system. Stimulating electrodes (two 0.5-cm^2 silver plates; 1-cm

186   apart) were placed over the median nerve, on the right side, at the wrist level (cathode proximal to

187   the spinal cord), and they were connected with shielded cables to the electrical stimulator (DS7A,

188   Digitimer Ltd, Hertfordshire, UK) located outside the MEG room. Percutaneous electrical stimuli (1-ms

189   duration) were first delivered in order to evaluate PT. The intensity was increased progressively until

190   the subject felt paraesthesia in the hand (cutaneous field of median nerve). The intensity was then

191   decreased and increased 3 to 5 times successively, in order to determine precisely the minimal

192   intensity for paraesthesia and local sensation below the stimulating electrodes. During recordings,

193   the stimulation intensity was set at 1.5, 3, 6 and 9 x PT; the maximum intensity (9 x PT) was described

194   by all subjects as unpleasant but not painful. The participants were instructed to stay as relaxed as

195   possible during recordings, not moving, no swallowing and not clenching the jaw. Cameras and

196   microphones were installed in the MEG room to maintain the contact with the subjects; videos and

197   discussions were not recorded.

198   The protocol included 8 recording sessions during which the subjects were asked to fix a cross

199   on the wall in front of them and to limit eye blinks. They were also instructed not to count the stimuli,

200   which interferes with SEP size (Mauguière *et al.*, 1997). Each recording session started with a 5-s

201   resting state acquisition (without stimulation) before triggering stimuli using a sequencer developed

202   in Matlab® (The MathWorks, Inc., Natick, MA, USA), which delivered time-locked triggers to the

203   electrical stimulators and synchronised event markers to the EEG-MEG acquisition system. Each

204   session consisted of 300 median nerve stimulations delivered with interstimulus interval (ISI)

205   randomly set between 500 and 600 ms (on average 555.8 ms). This ISI exceeds the time needed for

206   EEG and MEG signals to return to baseline after stimulation; no significant changes were observed

207   after 200 ms *i.e.*, within the time for somatosensory integration (Mauguière *et al.*, 1997; Mauguiere,

208   2005; Fig. 1AB). Moreover, it has been reported that stimulus rates of up to 8 Hz can be used without

209   significant loss in detectability of most components (Pratt *et al.*, 1980) and that P20/N20 is not

210   sensitive to ISI duration (Forss *et al.*, 1995; Mauguière *et al.*, 1997). Much less is known about late

211   components, and P100/N100 in particular, but it was necessary to keep the same procedure for valid

212   correlation analysis between the different components and the cortical areas activated; the

213   stimulation frequency between 1.6 and 2 Hz was a good compromise between optimal ISI duration

214   and total duration of recordings (for subject comfort). Stimulation intensity was kept constant during

215   one recording session and randomly changed from one session to another. Four intensities were

216   tested (1.5, 3, 6 and 9 x PT) and 2 recording sessions were performed at each intensity. Thus, 8

217   recording sessions (2 runs x 4 stimulation intensities) were performed and we collected a total of 600

218   conditioned signals at each of the 4 intensities tested. Including installation time, the total duration of

219   the EEG/MEG experiment was about 2 hours, plus 15 minutes for MRI.

220   **Anatomical MRI**

221   MRI was performed to obtain anatomical brain images for each participant (Magnetom TRIO

222   3T, Siemens Munich, Germany; CENIR, Brain Institute, Pitié-Salpêtrière Hospital, Paris, France). The

223   MRI images were obtained following a protocol adapted for MEG experiments: T1 weighting MPRAGE

224   sagittal orientation, flip angle = 9 °, TE = 2.22 ms, TR = 2,400 ms, TI = 1,000 ms, voxel size = 0.8 x 0.8 x

225   0.8 mm, matrix = 320 x 300, 256 contiguous slices. To avoid subject magnetisation, MRI acquisition

226   was performed after EEG-MEG acquisitions. Images were segmented using FreeSurfer

227   (https://surfer.nmr.mgh.harvard.edu) to reconstruct brain images that were used to localise the

228   source activity in each individual. During segmentation, Freesurfer registered the individual cortical

229   surfaces in 3 atlases (Desikan-Killiany, Destrieux, Brodmann). These atlases are implemented in

230   Brainstorm software used for the source analysis (Tadel *et al.*, 2011, 2019). The anatomical landmarks

231   (nasion, LPA, RPA, the anterior and posterior commissures and an inter-hemispheric point) were

232   manually defined on the MRI images.

233   **Time series' analysis**

234   *Preprocessing*. MEG time series were first filtered from external noises using MaxFilter (Elekta

235   Neuromag, Helsinki, Sweden). The EOG was then used to detect eyes blink artifacts in both EEG and

MEG signals. Independent component analysis (ICA; Fieldtrip toolbox, Matlab®) was performed to remove the EEG/MEG components that had the largest significant correlation coefficient with EOG. Then, ECG was used to detect and remove heart artifacts in MEG signals using principal component analysis (PCA; dataHandler, a software developed by the EEG/MEG centre of CENIR, Brain Institute, Pitié-Salpêtrière Hospital, Paris, France).

Epoching and averaging. We visually checked for the appropriate removal of ocular and cardiac signals (EOG, ECG), the absence of edge effects that could occur during signal correction, and the absence of electromyographic activity from other sources (facial and/or cranial muscles) interfering with EEG/MEG signals. Then, EEG and MEG were epoched using a 500-ms window time-locked to stimulus: 100 ms before (-100 ms) and 400 ms after the stimulus. EEG and MEG epochs from each acquisition were averaged (averaging of 300 epochs/run of acquisition), and the mean epochs from the 2 runs obtained at the same intensity were then averaged. Figure 1 AB show the superimposition of the mean epochs obtained at the level of each MEG (Fig. 1A) and EEG sensors (Fig 1B) in one participant.

Figure 1 near here

Source analysis. The realistic head model based on the symmetric boundary element method (BEM) was used for the forward problem using OpenMEEG in Brainstorm (Matlab®; Kybic *et al.*, 2005; Gramfort *et al.*, 2010) which enables reliable source location, especially for EEG (Lanfer *et al.*, 2012; Antonakakis *et al.*, 2019). The BEM model was computed using the MRI of each individual to include the surfaces representing the boundaries between the tissues used in the model: scalp (head-air interface), outer skull (scalp-skull interface) and inner skull interface (interface between skull and brain, including cerebrospinal fluid). According to the guidelines in Brainstorm, we selected all the layers for EEG, and only the inner skull layer for MEG (giving rise to similar results as using all layer), and we used adaptative integration (more accurate solution). For each subject and intensity, a noise covariance matrix was calculated on the pre-stimulus time-window ranging from -100 to -30 ms (excluding the stimulus artifact) using the 600 epochs in the 2 runs of acquisition corresponding to

262   that subject and intensity. Mean MEG and EEG epochs (in each individual, at each intensity tested)

263   were then used to analyse the sources using weighted minimum norm estimation (wMNE) with

264   unconstrained source orientation (Hämäläinen & Ilmoniemi, 1994; Baillet *et al.*, 1999; Tadel *et al.*,

265   2011, 2019; Baillet, 2017). We obtained the time courses of 3 orthogonal dipoles. The norm of their

266   vectorial sum was then computed, yielding time courses of cortical current density. Finally, we

267   calculated the corresponding Z-scores with respect to pre-stimulus baseline (noise covariance

268   matrix).

269   ***Windows of analysis corresponding to early and late components.*** The time windows covering

270   the early (P20/N20) and late source components (P60/N60 and P100/N100) were determined

271   according to our previous results (Sangari *et al.*, 2016) and the grand average (19 participants) of the

272   time course of normalized (Z-scored) current densities in EEG and MEG. According to previous studies

273   (Allison *et al.*, 1991; Mauguiere, 2005; Passmore *et al.*, 2014), we selected the results over the left

274   primary somatosensory area (contralateral to stimulation site; Fig. 2AB), obtained at 6 x PT (selected

275   according to our preliminary analyses showing this intensity was optimal; see Results). The resulting

276   time windows to calculate the mean current density for each component were: 17 to 21.5 ms after

277   stimulus trigger for P20/N20, 48 to 71 ms for P60/N60, and from 72 to 99 ms for P100/N100. The Z-

278   scores of the mean current density during these time windows were extracted in each individual for

279   group analysis.

280   ***Identification of ROIs***. Z-scores of current densities calculated in each individual between -100

281   and 400 ms around stimuli, were spatially projected into the standard Montreal Neurological Institute

282   (MNI) template to visualise the mean location of mean source activities in the group (grand average).

283   ROIs were defined in light of MEG activity at 6 x PT during the time windows covering P20/N20,

284   P60/N60 and P100/N100, and were delineated according to the Desikan-Killiany and Brodmann

285   atlases implemented in Brainstorm (premotor and SII areas were manually defined according to

286   Brodmann areas). The resulting atlas was used to compute Z-scores in corresponding cortical regions

287 in each individual according to their own anatomies (the atlas was projected onto individual MRIs),

288 during early and late SEPs.

289 **Statistical analysis**

290 We identified a total of 21 ROIs over the left (contralateral to the stimulation site) and right

291 (ipsilateral) hemispheres for the 2 modalities of recordings (same ROIs for EEG and MEG). We thus

292 performed a Bonferroni correction to determine the minimum Z-score ($\geq$ 4.02) to consider for

293 statistical significance (Figs. 2C-H and 3).

294 Linear mixed models were built with subjects as random effect and modality (MEG, EEG),

295 intensity (the 4 intensities tested), ROI (the 13 considered as significantly activated after Bonferroni

296 correction), component (P20/N20, P60/N60 and P100/N100) as fixed effects. Age and perceptual

297 threshold were also tested as co-variables. We made sure that the underlying assumptions

298 (normality, homoscedasticity and absence of outliers) were valid and *p*-values were calculated after

299 false discovery rate [FDR] correction. According to the results of the model, *post hoc* pairwise

300 analyses were performed using Student's t-tests on least-squares means of normalized current

301 densities (Z-scores).

302 We also investigated the correlations between SEP components and between ROIs during each

303 component. More specifically, we assessed the relationship between Z-scores corresponding to the

304 same ROI but different SEP components using Spearman's rank correlation coefficient. A threshold of

305 r = 0.7 was chosen both to select high intensity correlation and take into account multiple testing of

306 correlations (conservative Bonferroni correction). Partial correlations were processed to determine

307 ROIs which activity were closely linked between groups of regions. Lastly, we performed cluster

308 analysis using classification methods based on local singular value decomposition.

309 Statistical analyses were performed with JMP software® (SAS Inc., Cary, NC, USA). All tests were

310 2-sided. A *p*-value $\leq$ 0.05 was considered statistically significant. Data were reported as mean $\pm$ 1 SE

311 for continuous variable and as frequency (%) for categorical variables. For better readability, all tests

312 and parameters are specified in Results.

313

314

RESULTS

Figure 1 shows MEG and EEG raw data obtained at 6 x PT from one representative participant, with the superimposition of the mean epochs (Fig. 1AB) and their mean at the level of each sensor over the scalp (Fig. 1CD). Figure 1EF shows the topography of the signal at 20, 60 and 85 ms *i.e.*, within the analysis windows corresponding to P20/N20, P60/N60 and P100/N100, respectively. For both MEG and EEG topographies, most activity manifested in the left side, contralateral to stimulation site, and during P60/N60. Specifically, parietal regions were primarily activated at 20 ms (P20/N20), and fronto-parietal ones at later latencies. Source analysis and Z-score normalisation of mean current density was performed in each individual for the following group analyses.

Figure 2 near here

Source imaging

Source analysis resulted in the estimation of mean current density each 0.33 ms, between -100 ms and 400 ms around stimulation, which was then transformed into Z-score for group analysis. Figure 2AB shows MEG (A) and EEG (B) Z-scores over the left SI area (post-central gyrus), around median nerve stimuli adjusted at 6 x PT; each black trace shows the Z-scores in each participant (n = 19) and the red trace, the mean Z-scores in the group. On average, peaks of activity occurred at about 22 and 35 ms after peripheral stimuli, corresponding to early SEPs < 40 ms, and activity slowly increased again at about 45 ms in MEG and 55 ms in EEG, until 100 ms in MEG and longer in EEG, corresponding to late SEPs > 40 ms.

Z-scores of the mean current density during the time windows covering P20/N20, P60/N60 and P100/N100 were extracted for each individual. Figure 2C-H shows the projection of MEG (C-E) and EEG (F-H) Z-scores in the common MNI space (only used for this grand average) in the 3 windows of

337 analysis, P20/N20 (C,F), P60/N60 (D,G) and P100/N100 (E,H). According to Bonferroni correction for

338 multiple comparisons, significant activity during P20/N20 was mostly observed over the left fronto-

339 parietal cortex in both MEG and EEG maps (Fig. 2C,F). At longer latency, during P60/N60 (D,G) and

340 P100/N100 (E,H), the mean activity over the left sensorimotor cortex was greater as compared to

341 P20/N20, and spread over prefrontal, interhemispheric and posterior parietal areas in the left

342 (contralateral) and right (ipsilateral to stimulation site) hemispheres; the spreading being greater in

343 EEG compared to MEG. The ROIs were then determined according to MEG activity (given its greater

344 spatial accuracy compared to EEG; Leahy *et al.*, 1998; Komssi *et al.*, 2004; Baillet, 2017) during

345 P60/N60 (greater activity as compared to P100/N100, compare Figs. 2D and 2E). Significant activity in

346 the left hemisphere (contralateral to stimuli) was thus found in SI, SII (parietal operculum in the

347 ceiling of the lateral sulcus, overlapping ventral part of areas 40 and 43), superior posterior parietal

348 cortex (sPPC), inferior posterior parietal cortex (iPPC), supramarginal area (SMG), posterior cingulate

349 cortex (PCC), superior temporal sulcus (STS), insula, and over motor and premotor areas including

350 the primary motor cortex (M1), the premotor cortex (PM) and the supplemental motor area (SMA).

351 In the right hemisphere (ipsilateral to stimuli), significant activity was found in SI, SII, sPPC, iPPC, PCC,

352 STS, M1, PM and SMA.

353   During P20/N20, the most significant MEG activity in Figure 2C was limited to the left

354 (contralateral) hemisphere with i) the central sulcus including in its posterior part, Brodmann's area

355 3a and b (part of SI) and, in its anterior part, Brodmann's area 4 (M1), ii) the sulcus at the intersection

356 between SI, sPPC and SMG, and iii) the upper part of the premotor areas. Similar results were

357 observed in EEG but the activity was broader over the same areas (SI, M1, sPPC and SMA; Fig. 2F).

358 During P60/N60, the mean MEG activity increased in the same areas (contralateral SI, M1, sPPC and

359 SMA) and was much clearer in SII, as well as in the other areas listed supra but to a lesser extent in

360 these areas as compared to SI, M1, sPPC, SMA and SII (Fig. 2D). The mean EEG activity was much

361 greater than MEG, and again much broader in the left contralateral hemisphere; the difference with

362 MEG was even greater in the right -ipsilateral- hemisphere (Fig. 2G). At longer latencies,

363   corresponding to P100/N100, we observed similar results as during P60/N60, but the mean MEG

364   activity was globally lower (Fig. 2E) while the mean EEG activity increased again and was even

365   broader.

366   *Figure 3 near here*

367   Mean normalised epochs in Figure 2AB indicate that there was a great interindividual

368   variability (Buchner *et al.*, 1995; Ahn *et al.*, 2015). For EEG data, 28.6 % of the total variance could be

369   explained by between-SEP component variability, 20.3 % by between-ROIs variability, 21.6 % by

370   between-subject variability, and the 29.6 % left by interactions which led to an interclass coefficient

371   (ICC) of 0.15. For MEG data, 31.0 % of the total variance could be explained by between-SEP

372   component variability, 10.7 % by between-ROIs variability, 26.2 % by between-subject variability, and

373   the 32.0 % left by interactions which led to an ICC of 0.16. Therefore, we further investigated which

374   regions were mainly activated in the group, by calculating the proportion of subjects with significant

375   source activity in the different ROIs (still according to the Z-score threshold after Bonferroni

376   correction). The sunburst charts in Figure 3 shows the hierarchical distribution of MEG (Fig. 3A) and

377   EEG data in the group (Fig. 3B). The first level of hierarchy corresponds to the brain regions, and the

378   second level, to the SEP components: the larger the segment at a given level of the hierarchy, the

379   greater the proportion of subjects with significant Z-score (> 75 % of the participants with significant

380   Z-scores in red and between 50 and 74 %, in white). The first result that came out from this analysis is

381   that significant source activity was more consistent across subjects in the contralateral hemisphere in

382   both MEG and EEG, as compared to ipsilateral hemisphere. Moreover, the reproducibility of the

383   results across subjects was greater in EEG as compared to MEG. In addition, Figure 3B shows that

384   EEG activity in the ipsilateral hemisphere was quite consistent across subjects at the latency of late

385   components.

386   *Table 1 near here*

387   Table 1 summarises the data illustrated in Figure 3 to better highlight the common results in

388   MEG and EEG source imaging. During P20/N20, significant activity was found in both modalities in

389 the contralateral SI, SII, M1, PM and SMG, and in PCC on both hemispheres. At longer latencies,

390 during late SEPs, the results of source imaging were consistent between the two modalities in the

391 contralateral hemisphere while in the ipsilateral hemisphere, common activity was mostly found only

392 in SII and PCC. In fact, ipsilateral EEG activity was almost entirely limited to the upper part of the

393 hemisphere (Fig. 2GH), with no real demarcation between functional regions. In the lateral part,

394 significant ipsilateral MEG activity could be observed at the group level in the central sulcus (SI-M1),

395 PM, sPPC and STS (Fig. 2E) but according to Figure 3A and Table 1, these results were not replicable

396 in the major part of the participants.

397   The results of source imaging thus indicate that stimulus-induced activity during P20/N20

398 mostly occurred in contralateral SI, SII, M1, PM and SMG, and in PCC on both hemispheres. These

399 regions were still activated at longer latencies, during late SEPs, P60/N60 and P100/N100, which are

400 characterised, compared to P20/N20, by activity in contralateral SMA, sPPC, iPPC, STS and insula, and

401 ipsilateral SII. Video of source imaging (Supplemental material) reveals that the mean MEG activity in

402 the group started 18 ms after stimuli, at the level of the central (SI-M1), pre-central (premotor areas)

403 and post-central sulci (junction between SI, sPPC and SMG). Then, activity in SII and both contra- and

404 ipsilateral PCC occurred at 19-20 ms. At 22-23 ms, the activity decreased until 28 ms when it re-

405 increased again in the same areas as during P20/N20 with greater and more obvious activity in

406 contralateral PM, SII, sPPC, iPPC, STS and insula. Interestingly, ipsilateral MEG activity (right

407 hemisphere) in SII started at about 28 ms, being particularly clear at 30 ms, decreasing at about 38

408 ms, and re-increasing again about 56 ms, for being particularly significant between 62 and 97 ms.

409 Regarding EEG, activity mostly started at about 19 ms in contralateral central and pre-central sulci,

410 reaching sPPC at 20 ms, and then increased and spread in other contralateral areas until 38 ms, when

411 it decreased. It mostly re-increased again at about 60 ms for decreasing a bit at about 97 ms. In the

412 ipsilateral hemisphere, EEG activity was much broader than MEG. If we focus our attention on

413 ipsilateral SII, EEG activity started at 29 ms, and was more significant at 59 ms until the end of the

414 video. To sum up, the video indicates that the central sulcus is the first area to be activated during

415   P20/N20 but activity in SII, PM, SMG and PCC on both sides quickly occurred within the duration of

416   the time window for P20/N20. Then, activity in sPPC, iPPC, STS, insula and ipsilateral SII starts at

417   about 30 ms and was still observed during late SEPs, P60/N60 and P100/N100. Therefore, and even if

418   the activity decreased between early and late SEPs, all the cortical areas engaged in SEPs were

419   activated at 30 ms.

420   In order to further investigate the characteristics of late components and the respective role of

421   cortical areas in these responses, compared to P20/N20, we investigated the influence of stimulus

422   intensity on the responses over these ROIs (contralateral SI, SII, M1, PM, SMA, SMG, sPPC, iPPC, STS,

423   PCC, insula and ipsilateral PCC and SII).

424   ***Figure 4 near here***

425   **Influence of stimulus intensity**

426   On average, PT was 58.6 ± 3.7 µA, ranging from 37 to 95 µA (median value = 58 µA). Even if

427   particular care was taken to estimate precisely PT in each individual, the measure depended on their

428   concentration and their investment. Moreover, it has been reported that SEP amplitude increases

429   with age (Desmedt & Cheron, 1980, 1981; Kakigi & Shibasaki, 1991; Huttunen, 1995; Hagiwara *et al.*,

430   2014). We did not find any significant influence of PT on stimulation-induced cortical activities (linear

431   mixed model, *p*-value = 0.08). The influence of age did not reach the level of statistical significance

432   (*p*-value = 0.06) likely due to the fact that most of the participants were under 30 (14/19

433   participants). Lastly, a gender effect has also been reported in previous studies, especially in EEG due

434   to distinct volume conductor between males and females (MEG being not influenced by this

435   parameter; Huttunen *et al.*, 1999). However, given the number of subjects (13 females vs. 6 males)

436   and the number of parameters in the model, the comparison was not valid. However, we observed

437   higher values in females than in males, especially in EEG data (not in MEG). Even if the size of our

438   study group did not allow to further investigate these parameters (age and gender effect), it is

439   interesting that we were able to find similar characteristics as those reported in previous studies on

440   larger study groups.

441   Figure 4 illustrates the Z-scores of mean MEG (A,C,E) and EEG (B,D,F) current density in the

442   group, according to the intensity of the median nerve stimuli (x PT), in contralateral (c.) SI, SII, M1,

443   PM, SMA, SMG, sPPC, iPPC, STS, PCC, insula and ipsilateral (i.) PCC and SII, during the time window

444   corresponding to the 3 components P20/N20 (AB), P60/N60 (CD) and P100/N100 (EF). In all

445   conditions, Z-score systematically increased between 1.5 and 3 x PT (except in c.PM at the latency of

446   P20/N20 in MEG). Further increase in stimulus intensity mostly led to further increase in Z-score

447   except at the level of SMA in MEG P20/N20; Fig. 4A), or decrease at 6 x PT and re-increase at 9 x PT

448   (*e.g.*, in SI, M1, SMA and sPPC using EEG; Fig. 3A) or still increase at 6 x PT and decrease at 9 x PT

449   (*e.g.*, in SII using EEG at the latency for P20/N20 and P60/N60; Fig. 3AC).

450   ***Figure 5 near here***

451   ***Table 2 near here***

452   Repeated-measures linear mixed-effects model was computed to evaluate the influence of the

453   intensity (1.5, 3, 6, 9 x PT) on the Z-score of mean current density taking into account the recording

454   modality (MEG, EEG), the ROIs (contralateral SI, SII, M1, PM, SMA, SMG, sPPC, iPPC, STS, PCC, insula

455   and ipsilateral [i.] PCC and SII) and the component (P20/N20, P60/N60, P100/N100). Adjusted R^2 was

456   0.98 and all fixed effects and their interactions were significant: FDR-corrected *p*-value < 0.001 for all

457   regressors and interactions except for that between intensity, recording modality and component for

458   which *p*-value < 0.05. Least-squares means of Z-scores were then used to illustrate the interactions

459   between factors, which best represents the model prediction (taking into account all factors) and

460   gives a much greater readability of the influence of the stimulus intensity on MEG and EEG activities

461   and their location during early and late components. *Post hoc* pairwise comparisons of least-squares

462   means were performed using Student's t tests. Figure 5 shows that least-squares means were

463   significantly greater for EEG than for MEG above 3 x PT (Fig. 5A; *p*-value < 0.001) and much more

464   similar between late components (P60/N60, P100/N100) compared to early one (P20/N20; Fig. 5CD);

465   differences between P60/N60 and P100/N100 being mostly non-significant contrary to those

466   between P20/N20 and the two late components (see *p*-values in Table 2). The similarity between late

467 components is also shown in Figure 5B; differences between late component being non-significant

468 (*p*-value = 0.17 in MEG and 0.74 in EEG). This figure also indicates that during P20/N20, there was no

469 significant differences between MEG and EEG (*p*-value = 0.1). The model thus indicates greater

470 activity in EEG than in MEG at intensity ≥ 3 x PT but the difference between the two modalities

471 mostly manifests during late components; MEG and EEG activity being comparable during P20/N20.

472 Furthermore, the model reveals similar influence of stimulus intensity on late components but

473 different from P20/N20.

474   ***Figure 6 near here***

475   Figure 6 illustrates the interaction between the recording modalities, the stimulus intensity

476 and the ROIs. According to the model, MEG activity increased mostly similarly between 1.5 and 6 x PT

477 whatever the ROIs (Fig. 6A), but there was a steep increase in EEG activity between 1.5 and 3 x PT

478 (Fig. 6B). This result is also illustrated in Figure 5A showing that the slope between 1.5 and 3 x PT is

479 greater for EEG compared to MEG. Between 6 and 9 x PT, both MEG and EEG activities still increased

480 but to a much lesser extent, especially in MEG, compared to the difference between 3 and 6 x PT.

481 This result suggests that SEPs plateaued at intensity ≥ 3x PT in MEG and ≥ 6 x PT in EEG; see also

482 Figure 5A and the non-significant differences in MEG, between 3 and 6 (*p*-value = 0.06) and between

483 6 and 9 x PT (*p*-value = 0.15). After *post hoc* pairwise comparisons, the conditions with similar results

484 were clustered and we found similar grouping in MEG and EEG including: i) at 3 x PT, PPC-SI and

485 SMG-M1, ii) at 6 x PT, SI-M1-SMG, and iii) at 9 x PT, SI-M1.

486   ***Figure 7 near here***

487   Figure 7 illustrates the interaction between the recording modalities, the components and the

488 ROIs. Results at the latency of late components are more similar than those at the latency of

489 P20/N20, especially in EEG (Fig. 7B; as illustrated in Fig. 5CD). Moreover, Figure 7 shows comparable

490 results in some ROIs depending on the component and the recording modalities. We thus compared

491 the clusters after *post hoc* pairwise comparisons to identify ROIs with comparable results in both

492 MEG and EEG: i) at the latency of P20/N20, SI-M1-SMG, and ii) at the latency of P60/N60, SI-M1 and

493   STS-i.SII; we did not find any common cluster at the latency for P100/N100.

494   Whether for stimulus intensity or component, similar results were observed between S1, M1

495 and SMG suggesting that activities within these areas were likely particularly linked. To further

496 investigate the relationships between ROIs during early and late components, we performed

497 correlation analysis at the optimal intensity 6 x PT (for both MEG and EEG, and in most ROIs).

498   **Correlation between SEP components and between ROIs**

499   Correlation analyses were performed to evaluate the statistical links between ROIs and SEP

500 components when stimulus intensity was set at 6 x PT. Regarding the correlation between early and

501 late components, we did not find any significant correlation in MEG activities between early and late

502 components in ROIs significantly activated. In EEG, we found only significant correlation ($r > 0.7$)

503 between P20/N20 and P100/N100 at the level of i) STS (P100/N100) and sPPC (P20/N20; *p*-value <

504 0.0001), ii) STS (P100/N100) and iPPC (P20/N20; *p*-value < 0.001), iii) PCC (P100/N100) and M1

505 (P20/N20; *p*-value < 0.001), iv) STS (P100/N100) and sPPC (P20/N20; *p*-value < 0.001), v) STS

506 (P100/N100) and M1 (P20/N20; *p*-value < 0.001), and vi) STS (P100/N100) and SI (P20/N20; *p*-value <

507 0.001).

508   We also studied the link between ROIs within each component using partial correlation which

509 measured the degree of association between ROIs considering the other ones. For MEG-P20/N20, we

510 found significant link between SI and M1, and M1 and PM. For MEG-P60/N60, we found significant

511 correlations between M1, PM, SII; SMG was also linked to SI and to SII but activity in SI and SII were

512 not significantly correlated. Last, for MEG-P100/N100, we found significant correlations between SI

513 and M1, SI and SMG, M1 and PM, M1 and sPPC, and between PM and SMA.

514   For EEG-P20/N20, we still found significant correlation between SI and M1. We also found

515 significant link between activities in SI and SMG, SII and SMG, sPPC and iPPC, and STS and iPPC. For

516 EEG-P60/N60, we found significant correlation between SI and SMG, SI and M1, M1 and PM, PM and

517 SII, and SII and SMG. Last, for EEG-P100/N100, we found again significant correlations between SI

518 and SMG, SI and M1, M1 and PM, and SII and insula.

519   This analysis confirms that the correlation between early and late components is sparse and,

520   most importantly, that there is very limited or even no link between early and late (only some

521   between P20/N20 and P100/N100). Accordingly, the most reliable linked MEG/EEG activities

522   between ROIs include SI-M1 and M1-PM at the latency of P20/N20 and P100/N100. P60/N60 is

523   distinguished by other correlations including for the most reliable M1-PM-SII, SI-SMG, and SII-SMG.

524   At the latency of P20/N20, EEG activities in associative cortices were significantly linked (sPPC-iPPC,

525   STS-iPPC).

526   **Clusters of cortical activity**

527   Last part of the statistical analysis consisted of running classification methods based on a local

528   singular value decomposition followed by a clustering algorithm which divided iteratively the clusters

529   of variables (SEP components and ROIs, stimulus intensity at 6 x PT) and reassigned the variables to

530   clusters until it was not possible to split the clusters. First interesting result was that P20/N20,

531   P60/N60 and P100/N100 constituted distinct clusters which further supports that early and late

532   components were not linked. Secondly, we found 4 clusters in both MEG and EEG. At the latency of

533   P20/N20, we found common MEG and EEG activity in SI, M1 SMG and PM as the most representative

534   variables in the cluster. Regarding P60/N60, we found one cluster in MEG and two in EEG. The

535   common cluster included SI, M1, PM and SII and the second cluster in EEG included associative

536   cortices (iPPC, sPPC, SMG and STS). Lastly, at the latency of P100/N100, we found one common

537   cluster involving SI, M1, SMG and PCC; the second cluster only observed in MEG included STS and

538   insula. These results indicate that MEG/EEG main activity was commonly observed in SI and M1

539   during early and late SEPs without any link between components. The three components were

540   distinct by activity in PM during P20/N20 and P60/N60, SII has particularly contributed to P60/N60,

541   and PCC to P100/N100.

542   **DISCUSSION**

543   This first aim of the study was to investigate the temporality of cortical activation maps after

median nerve stimulation at the wrist level. It is shown that the contralateral primary sensorimotor area (SI-M1) in the central sulcus is first activated (18 ms) and rapidly, still during the time window covering P20/N20, activity in contralateral SMG, PM, SII and both contra- and ipsilateral PCC has occurred. At longer latency (> 30 ms) and during P60/N60 and P100/N100, activity in these areas was combined to activity in contralateral multisensory associative cortices (sPPC, iPPC, STS, insula) and SMA, and in ipsilateral SII.

The second aim was to investigate the relationship between stimulus intensity and source activities in the different ROIs to further identify specific features of late SEPs as compared to P20/N20. The first interesting finding included similar results in MEG and EEG during P20/N20 but not during late SEPs. Furthermore, while all responses plateaued at intensity between 3 and 6 x PT, the relationship between stimulus intensity and late responses was similar but different from P20/N20. Lastly, correlation and cluster analyses did not reveal any significant link between early and late components. However, clustered activity in the primary sensorimotor area (SI-M1) was consistently observed during the early and late components, each one being characterised by added activity in PM and SMG during P20/N20, in SII and PM during P60/N60 and in SMG and PCC during P100/N100. Late SEPs were also characterised by another cluster including multisensory associative cortices (iPPC, sPPC, SMG, STS and insula).

Extra-somatosensory activity during P20/N20

It has been well established that P20/N20 is generated in the contralateral primary somatosensory cortex, particularly in areas 3b and 1, in response to cutaneous inputs from median nerve stimulation (Allison *et al.*, 1991; Hashimoto *et al.*, 2001; Valeriani *et al.*, 2001; Mauguiere, 2005; Baumgärtner *et al.*, 2010; Papadelis *et al.*, 2011). Studies using source imaging have consistently revealed that cortical activity is maximal in the central sulcus (Antonakakis *et al.*, 2019; Rezaei *et al.*, 2021). In the present study, maximal activity was also found in the central sulcus at 20 ms (Supplemental material 1). However, to a smaller extent but statistically significant, activity in pre- and post-central sulci was generated at the same time.

570   P20/N20 activity was quantified in ROIs defined according to Desikan-Killiany and Brodmann

571   atlases projected onto individual MRIs, within a time window covering the full duration of the

572   component (16-22 ms) while in most studies peak activity (~20 ms) was used to quantify the cortical

573   activity. Time-window analysis (instead of peak activity) was chosen to enable reliable comparison

574   between early and late components since the latter are characterized by slow signal with peak

575   activity extremely variable from one individual to another (see Fig. 2AB). On one hand, calculating

576   activity within the full-time window increases the signal-to-noise ratio and enables a better

577   extraction of stimulus-induced cortical activity from background activity and noise. On the other

578   hand, it takes into account a broader activity, possibly exceeding that in area 3b characterised at the

579   peak activity. However, this is unlikely since cortical activity at the peak latency for N20 and P22 has

580   been respectively localised in area 3b and area 1 (Hashimoto *et al.*, 2001; Mauguiere, 2005;

581   Baumgärtner *et al.*, 2010; Papadelis *et al.*, 2011) and here we found that activity in the pre-, post-

582   and central sulci was generated simultaneously.

583   ROIs and statistical analyses revealed that P20/N20 was characterised by activity in SI, M1, PM

584   and SMG (the two later ROIs being likely associated to activity in pre- and post-central sulci,

585   respectively). Importantly, results in MEG and EEG were similar. EEG is indeed sensitive to both

586   tangential and radial dipoles while MEG is less sensitive but not fully blind to radial sources (Leahy *et*

587   *al.*, 1998). Accordingly, a possible greater localisation error in EEG, compared to MEG, is still matter

588   of debate, being between 3 mm and 1.5 cm according to authors (Leahy *et al.*, 1998; Komssi *et al.*,

589   2004; Baillet, 2017). However, the error in EEG is reduced when using high density EEG (32 to 256

590   electrodes; error decreasing when using more than 32 electrodes), individual MRI for more precise

591   information of head anatomy and sophisticated source localisation algorithms (Baillet *et al.*, 2001;

592   Komssi *et al.*, 2004; Michel *et al.*, 2004; Michel & Murray, 2012; Michel & Brunet, 2019; Michel & He,

593   2019).

594   The central sulcus includes part of M1 (anterior bank) and areas 3a and 3b of SI (posterior

595   bank); its deep part being a combination of both M1 and area 3a. It has been established that

596   P20/N20 is generated in the posterior bank of the central sulcus corresponding to area 3b (Allison *et*

597   *al.*, 1991) but variations in central sulcus anatomy may cause unusual SEP topographies (Legatt &

598   Kader, 2000) and likely the high inter-individual variability, thus limiting the precise location of source

599   activity. While M1 and SI ROIs did not overlap (pre- and post-central gyri, respectively; sparing the

600   deep part of the central sulcus) our approach does not allow to determine whether activity in M1

601   during P20/N20 was real or due to diffusion of activity generated in area 3b (Schoffelen & Gross,

602   2009). Alternatively, one would argue that the activation of M1 could be related to the activation of

603   motor axons at the peripheral nerve level, but this is unlikely since i) the antidromic volley in motor

604   axons is limited to spinal motoneurons and could only induce proprioceptive afferent inputs in

605   response to muscle twitch, in addition to the direct electrical volley in sensory afferents (Pierrot-

606   Deseilligny & Burke, 2005) and ii) we found activity in M1 even at 1.5 x PT *i.e.*, below MT. Moreover,

607   activity in precentral gyrus was clearly observed from 30 ms (Supplemental material) and the close

608   link between SI and M1 activities was systematically observed during the 3 components while activity

609   during the 3 components was not correlated. This suggests that the activity quantified in M1 ROI was

610   likely not of the same origin from one component to another, nor that in SI given the temporality of

611   activity changes in both ROIs.

612   Can we argue that P20/N20 activity was only limited to area 3b? Several lines of evidence do

613   not fully support this assumption. First, we cannot fully discard a contribution of M1 since it has been

614   shown to be activated during P20/N20 in animal models (Lemon, 1981; Tanji & Wise, 1981; Peterson

615   *et al.*, 1995) and transcranial magnetic stimulation in humans has revealed that SI and M1 are co-

616   modulated by somatosensory inputs (Schabrun *et al.*, 2012). Moreover, high frequency oscillations

617   during P20/N20 are partly due to presynaptic activity in thalamo-cortical projections (Urasaki *et al.*,

618   2002; Gobbelé *et al.*, 2003, 2004; Jaros *et al.*, 2008; Sakura *et al.*, 2009) which is further supported by

619   subcortical source analysis which revealed the contribution of the lateral ventro-parietal nuclei of the

620   thalamus (relay of the somatosensory afferents to SI and SII; Rezaei *et al.*, 2021). Lastly, we found

621   activity in pre- and post-central sulci likely associated to activity in premotor areas (PM) and

622   associative cortex (SMG).

623   **Characteristics of late components**

624   Late components were characterised by different clusters than those identified during

625   P20/N20 which is consistent with the absence of correlation between the 3 components, especially

626   between P20/N20 and P60/N60, and the fact that I/O relationships were different between early and

627   late components. The late components have been studied to a much smaller extent compared to

628   P20/N20 and little is known on their origin and they are not used in clinical routine. To date, the

629   knowledge is limited to the implication of contralateral SII, which is thus considered as the region of

630   late cortical responses to peripheral nerve stimuli (Mauguiere, 2005). Source imaging in the present

631   study has revealed a much broader cortical activity during late components, involving a more

632   complex cortico-cortical sensorimotor network. Moreover, we found significant activity in the

633   ipsilateral SII using both MEG and EEG, as previously reported using intracerebral recordings which

634   has been attributed to deep source (Barba *et al.*, 2002; Mauguiere, 2005).

635   Besides the location of dipoles or magnetic fields, several studies aimed at investigating the

636   influence of stimulus intensity on SI/SII activity or P20/N20-P60/N60 strength (I/O relationship), to

637   compare the characteristics of early and late responses. All studies reported a plateaued effect

638   affecting SI/P20/N20 only (Gerber & Meinck, 2000; Torquati *et al.*, 2002) or both SI/P20/N20 and

639   SII/P60/N60 (Huttunen, 1995; Lin *et al.*, 2003) or only SII response (Jousmäki & Forss, 1998). Because

640   the stimulus intensity was not normalised or normalised but not the same way from one study to

641   another, and even in the same study, it is difficult to determine exactly the minimum intensity for

642   saturation but plateau was reported between 2-3 x PT and 1 x MT. In the present study, intensity was

643   normalised to PT (Fukuda *et al.*, 2007) and we investigated the I/O relationship taking into account

644   the different ROIs. First of all, we found that the main increase occurred between 1.5 and 3 x PT,

645   which was more marked for EEG than for MEG. Plateau effect was much clearer for P20/N20 than for

646   late components, occurring between 3 and 6 x PT (Fig. 5BC). We did not check MT in our

647   experimental group but in previous studies in our laboratory, we found MT in median nerve is about

648 4 x PT, ranging from 3 to 6 x PT. Therefore, plateaued effect manifested at intensity ≥ 1 x MT, as

649 previously reported for P20/N20. This was true in almost all areas with less difference between Z-

650 scores at intensity ≥ 6 x PT in MEG and ≥ 3 x PT in EEG (Fig. 6AB), except SII whose response

651 decreased with intensity > 6 x PT. Similar decrease in SII response with stimulus intensity has already

652 been reported but without specifying the timing (Torquati *et al.*, 2002). In line with the fact that

653 saturation was observed mainly during P20/N20, as reported previously (Huttunen, 1995; Gerber &

654 Meinck, 2000; Torquati *et al.*, 2002; Lin *et al.*, 2003), we found similar I/O relationship for P60/N60

655 and P100/N100 but different for P20/N20. Indeed, both P60/N60 and P100/N100 mostly still

656 increased with stimulus intensity > 3 x PT, but with slower slope than between 1.5 and 3 x PT (Fig.

657 5CD). The fact that we did not observe a clear plateau effect is not contradictory from previous

658 studies given the great variability of SEP responses (Huttunen, 1995; Jousmäki & Forss, 1998; Lin *et*

659 *al.*, 2003).

660   Five clusters of ROIs but different from one component to another could be identified. We

661 consistently found SI and M1 in one cluster for each component, which might be due to leakage

662 activity between these two very close areas (Schoffelen & Gross, 2009). However, since there was no

663 correlation between components, there is a possibility that activity in these 2 ROIs is not of the same

664 origin from one component to another (activity mostly in central sulcus during P20/N20, *plus*

665 enhanced activity in pre- and post-central gyri at latency ≥ 30 ms). Moreover, the cluster including SI-

666 M1 involves other areas as main variables but different from one component to another: PM and

667 SMG during P20/N20, SII and PM during P60/N60, SMG and PCC during P100/N100. The 2 other

668 clusters involved multisensory associative cortex with iPPC, sPPC, SMG and STS during P60/N60, and

669 STS and insula during P100/N100. These results suggest that late components are likely not

670 characterised by activity in SII only, but might involve more complex cortico-cortical interactions,

671 including the primary and secondary somatosensory areas, motor, premotor and multisensory

672 associative cortices in the contralateral hemisphere and ipsilateral SII.

673   **Cortical network(s) underlying late SEPs and functional implications**

674   EEG and MEG source imaging has revealed a much broader activity at cortical level than

675 reported previously, both during early and late SEPs. While it is globally admitted that P20/N20 is

676 limited to activity of area 3b neurons, the present study has revealed activity in pre- and post-central

677 sulci likely linked to activity in PM and SMG ROIs. Similarly, late components are not limited to

678 activity in SII but are the result of activity in the same areas as during P20/N20, *plus* SII (both

679 hemispheres) and multisensory associative cortices (iPPC, sPPC, STS, PCC, insula). While the time

680 resolution of functional MRI does not allow to distinguish activity between early and late

681 components, the mapping of hemodynamic responses after electrical median nerve stimulation and

682 mechanical stimulation of hand skin (Boakye *et al.*, 2000) fully matches the present results of

683 EEG/MEG source imaging.

684   Besides different source locations, early and late components exhibited different sensitivity to

685 stimulus intensity, suggesting the contribution of different neural networks with distinct I/O

686 relationships. Brain connectivity has been assessed after median nerve stimulation but the studies

687 focused on SI, SI-M1 or the resulting change in default mode and fronto-parietal networks has been

688 studied (Tecchio *et al.*, 2005; Porcaro *et al.*, 2013; Mayhew *et al.*, 2014; Kobayashi *et al.*, 2015).

689 Further studies need to be undertaken to evaluate the dynamical functional connectivity between

690 brain areas activated by median nerve stimulation we reported here, and previously using fMRI

691 (Boakye *et al.*, 2000), specifically in the different clusters of activity we identified. Such investigations

692 would also help to i) establish whether SII receive a copy of afferent inputs through direct

693 thalamocortical projections and/or indirectly via SI and ii) elucidate the roles of these 2 areas in

694 somatosensory processing at the cortical level (Mauguiere, 2005; Klingner *et al.*, 2016). If both areas

695 were involved in the same network, one would expect the activity in both areas would be correlated

696 to some extent, which is not supported by the present study.

697   It is well established that SI is the first and main target of thalamocortical projections relaying

698 peripheral afferent inputs to cerebral cortex and M1, the main cortical output in motor system; the

699 interaction between both being mediated through associative cortex and sPPC in particular (Coquery,

700 2011). Both sPPC and iPPC receive multimodal sensory inputs and are involved in sensorimotor

701 control (feedback control), recognition, motor planning, executive and working memory, and motor

702 learning (Mesulam, 1998; Buneo & Andersen, 2006; Binkofski & Buccino, 2018; Tumati *et al.*, 2019).

703 Lastly, premotor areas, including SMA and PM, are involved in condition-action association, motor

704 planning, initiation and learning (Rizzolatti & Craighero, 2004; Binkofski & Buccino, 2006; Davare *et*

705 *al.*, 2006; Nachev *et al.*, 2008; Solopchuk *et al.*, 2016). All these areas take part in several neural

706 networks involved in the integration of sensory information to initiate multiple cognitive and

707 behavioral outcomes (Mesulam, 1998), which supports the results of EEG/MEG source imaging in the

708 present study. However, the identification of brain areas activated by somatosensory inputs is not

709 sufficient to understand how those inputs are processed at cortical level during motor and cognitive

710 functions. This also requires a better knowledge of their interactions and, particularly, the pathways

711 by which sensory information is mediated.

712 **Impacts for future studies and clinical investigations**

713 It is commonly accepted that somatosensory inputs to the cortex undergo early and late stages

714 of processing. This way, early and late SEPs have been often compared to better evaluate the

715 influence of somatosensory inputs and their gating in the different phases of movement (planning,

716 initiation and execution; Saradjian *et al.*, 2013; Mouchnino *et al.*, 2017). Although elegant and

717 particularly ingenious, this approach gives rise to results that should be considered with caution

718 given the great overlap in the brain areas involved in early and late SEPs and their possible

719 interaction. In line with this, in our previous study in patients with ALS (Sangari *et al.*, 2016), we

720 found that late SEPs were more altered than early SEPs, and their alteration was not correlated. The

721 present results further confirm that early and late SEPs reflect activity in different neural networks

722 involving sensorimotor and non-motor areas, and that their correlation, if anything, is low. However,

723 the comparison between early and late SEPs, during specific tasks and in pathological conditions,

724 should be performed using high density EEG allowing source imaging for accurate evaluation of brain

725 processing.

Conclusions

The present study revisits the origin of late SEPs. The focus was on P60/N60 and P100/N100 that we compared to *a priori* well-known P20/N20 component. Further investigations would be interesting to better understand the dynamics of brain processing, including intermediate components of SEPs; something solely possible using EEG/MEG source imaging which finally was only fewly used to investigate the early and late phases of brain processing of somatosensory inputs, to date. In addition, this study indicates that the clinical use of SEPs is particularly limited given the potential information on brain functions such an approach can give, not only on the transmission along the sensory pathway. Further research on signal processing, comparing the results of clinical SEP investigation in routine (with simple setup) and complex laboratory EEG/MEG source imaging (difficult to implement in routine), would be particularly interesting to evaluate the respective role of the different networks underlying early and late SEPs, in order to propose new biomarkers of brain functions and complex processing, that would enable to implement the use of late SEPs in clinics, to evaluate brain functions in patients.

REFERENCES

Ahn, S., Kim, K., & Jun, S.C. (2015) Steady-State Somatosensory Evoked Potential for Brain-Computer Interface-Present and Future. *Front Hum Neurosci*, **9**, 716.

Allison, T., McCarthy, G., Wood, C.C., & Jones, S.J. (1991) Potentials evoked in human and monkey cerebral cortex by stimulation of the median nerve. A review of scalp and intracranial recordings. *Brain*, **114 (Pt 6)**, 2465–2503.

Antonakakis, M., Schrader, S., Wollbrink, A., Oostenveld, R., Rampp, S., Haueisen, J., & Wolters, C.H. (2019) The effect of stimulation type, head modeling, and combined EEG and MEG on the source reconstruction of the somatosensory P20/N20 component. *Hum Brain Mapp*, **40**, 5011–5028.

Baillet, S. (2017) Magnetoencephalography for brain electrophysiology and imaging. *Nat. Neurosci.*, **20**, 327–339.

Baillet, S., Garnero, L., Marin, G., & Hugonin, J.P. (1999) Combined MEG and EEG source imaging by minimization of mutual information. *IEEE Trans Biomed Eng*, **46**, 522–534.

Baillet, S., Riera, J.J., Marin, G., Mangin, J.F., Aubert, J., & Garnero, L. (2001) Evaluation of inverse methods and head models for EEG source localization using a human skull phantom. *Phys Med Biol*, **46**, 77–96.

Barba, C., Frot, M., Valeriani, M., Tonali, P., & Mauguière, F. (2002) Distinct fronto-central N60 and supra-sylvian N70 middle-latency components of the median nerve SEPs as assessed by scalp

topographic analysis, dipolar source modelling and depth recordings. *Clin Neurophysiol*, **113**, 981–992.

Baumgärtner, U., Vogel, H., Ohara, S., Treede, R.-D., & Lenz, F.A. (2010) Dipole source analyses of early median nerve SEP components obtained from subdural grid recordings. *J Neurophysiol*, **104**, 3029–3041.

Binkofski, F. & Buccino, G. (2006) The role of ventral premotor cortex in action execution and action understanding. *J Physiol Paris*, **99**, 396–405.

Binkofski, F. & Buccino, G. (2018) The role of the parietal cortex in sensorimotor transformations and action coding. *Handb Clin Neurol*, **151**, 467–479.

Boakye, M., Huckins, S.C., Szeverenyi, N.M., Taskey, B.I., & Hodge, C.J. (2000) Functional magnetic resonance imaging of somatosensory cortex activity produced by electrical stimulation of the median nerve or tactile stimulation of the index finger. *J Neurosurg*, **93**, 774–783.

Buchner, H., Adams, L., Müller, A., Ludwig, I., Knepper, A., Thron, A., Niemann, K., & Scherg, M. (1995) Somatotopy of human hand somatosensory cortex revealed by dipole source analysis of early somatosensory evoked potentials and 3D-NMR tomography. *Electroencephalogr Clin Neurophysiol*, **96**, 121–134.

Buchner, H., Fuchs, M., Wischmann, H.A., Dössel, O., Ludwig, I., Knepper, A., & Berg, P. (1994) Source analysis of median nerve and finger stimulated somatosensory evoked potentials: multichannel simultaneous recording of electric and magnetic fields combined with 3D-MR tomography. *Brain Topogr*, **6**, 299–310.

Buneo, C.A. & Andersen, R.A. (2006) The posterior parietal cortex: sensorimotor interface for the planning and online control of visually guided movements. *Neuropsychologia*, **44**, 2594–2606.

Coquery, J. (2011) *Neurosciences: Purves, Augustine, Hall, Lamantia, MacNamara, Willimans.*, 4e edn, Neurosciences et Cognition. de Boeck, Bruxelles.

Davare, M., Andres, M., Cosnard, G., Thonnard, J.-L., & Olivier, E. (2006) Dissociating the role of ventral and dorsal premotor cortex in precision grasping. *J Neurosci*, **26**, 2260–2268.

Desmedt, J.E. & Cheron, G. (1980) Somatosensory evoked potentials to finger stimulation in healthy octogenarians and in young adults: wave forms, scalp topography and transit times of parietal and frontal components. *Electroencephalography and Clinical Neurophysiology*, **50**, 404–425.

Desmedt, J.E. & Cheron, G. (1981) Non-cephalic reference recording of early somatosensory potentials to finger stimulation in adult or aging normal man: differentiation of widespread N18 and contralateral N20 from the prerolandic P22 and N30 components. *Electroencephalography and Clinical Neurophysiology*, **52**, 553–570.

Forss, N., Jousmäki, V., & Hari, R. (1995) Interaction between afferent input from fingers in human somatosensory cortex. *Brain Res.*, **685**, 68–76.

Fukuda, H., Sonoo, M., Kako, M., & Shimizu, T. (2007) Optimal method to determine the stimulus intensity for median nerve somatosensory evoked potentials. *J Clin Neurophysiol*, **24**, 358–362.

Gerber, J. & Meinck, H.M. (2000) The effect of changing stimulus intensities on median nerve somatosensory-evoked potentials. *Electromyogr Clin Neurophysiol*, **40**, 477–482.

Gobbelé, R., Waberski, T.D., Simon, H., Peters, E., Klostermann, F., Curio, G., & Buchner, H. (2004) Different origins of low- and high-frequency components (600 Hz) of human somatosensory evoked potentials. *Clin Neurophysiol*, **115**, 927–937.

Gobbelé, R., Waberski, T.D., Thyerlei, D., Thissen, M., Darvas, F., Klostermann, F., Curio, G., & Buchner, H. (2003) Functional dissociation of a subcortical and cortical component of high-frequency oscillations in human somatosensory evoked potentials by motor interference. *Neurosci Lett*, **350**, 97–100.

Gramfort, A., Papadopoulo, T., Olivi, E., & Clerc, M. (2010) OpenMEEG: opensource software for quasistatic bioelectromagnetics. *Biomed Eng Online*, **9**, 45.

Hagiwara, K., Ogata, K., Okamoto, T., Uehara, T., Hironaga, N., Shigeto, H., Kira, J., & Tobimatsu, S. (2014) Age-related changes across the primary and secondary somatosensory areas: an analysis of neuromagnetic oscillatory activities. *Clinical Neurophysiology: Official Journal of the International Federation of Clinical Neurophysiology*, **125**, 1021–1029.

Hämäläinen, M.S. & Ilmoniemi, R.J. (1994) Interpreting magnetic fields of the brain: minimum norm estimates. *Med Biol Eng Comput*, **32**, 35–42.

Hashimoto, I., Kimura, T., Iguchi, Y., Takino, R., & Sekihara, K. (2001) Dynamic activation of distinct cytoarchitectonic areas of the human SI cortex after median nerve stimulation. *Neuroreport*, **12**, 1891–1897.

Huang, M.-X., Song, T., Hagler, D.J., Podgorny, I., Jousmaki, V., Cui, L., Gaa, K., Harrington, D.L., Dale, A.M., Lee, R.R., Elman, J., & Halgren, E. (2007) A novel integrated MEG and EEG analysis method for dipolar sources. *Neuroimage*, **37**, 731–748.

Huttunen, J. (1995) Effects of stimulus intensity on frontal, central and parietal somatosensory evoked potentials after median nerve stimulation. *Electromyogr Clin Neurophysiol*, **35**, 217–223.

Huttunen, J., Wikström, H., Salonen, O., & Ilmoniemi, R.J. (1999) Human somatosensory cortical activation strengths: comparison between males and females and age-related changes. *Brain Research*, **818**, 196–203.

Jaros, U., Hilgenfeld, B., Lau, S., Curio, G., & Haueisen, J. (2008) Nonlinear interactions of high-frequency oscillations in the human somatosensory system. *Clin Neurophysiol*, **119**, 2647–2657.

Jousmäki, V. & Forss, N. (1998) Effects of stimulus intensity on signals from human somatosensory cortices. *Neuroreport*, **9**, 3427–3431.

Kakigi, R. & Shibasaki, H. (1991) Effects of age, gender, and stimulus side on scalp topography of somatosensory evoked potentials following median nerve stimulation. *Journal of Clinical Neurophysiology: Official Publication of the American Electroencephalographic Society*, **8**, 320–330.

Klingner, C.M., Brodoehl, S., Huonker, R., & Witte, O.W. (2016) The Processing of Somatosensory Information Shifts from an Early Parallel into a Serial Processing Mode: A Combined fMRI/MEG Study. *Front Syst Neurosci*, **10**, 103.

Kobayashi, K., Matsumoto, R., Matsuhashi, M., Usami, K., Shimotake, A., Kunieda, T., Kikuchi, T., Mikuni, N., Miyamoto, S., Fukuyama, H., Takahashi, R., & Ikeda, A. (2015) Different Mode of Afferents Determines the Frequency Range of High Frequency Activities in the Human Brain: Direct Electrocorticographic Comparison between Peripheral Nerve and Direct Cortical Stimulation. *PLoS One*, **10**, e0130461.

Komssi, S., Huttunen, J., Aronen, H.J., & Ilmoniemi, R.J. (2004) EEG minimum-norm estimation compared with MEG dipole fitting in the localization of somatosensory sources at S1. *Clin Neurophysiol*, **115**, 534–542.

Kybic, J., Clerc, M., Abboud, T., Faugeras, O., Keriven, R., & Papadopoulo, T. (2005) A common formalism for the integral formulations of the forward EEG problem. *IEEE Trans Med Imaging*, **24**, 12–28.

Lanfer, B., Scherg, M., Dannhauer, M., Knösche, T.R., Burger, M., & Wolters, C.H. (2012) Influences of skull segmentation inaccuracies on EEG source analysis. *Neuroimage*, **62**, 418–431.

Leahy, R.M., Mosher, J.C., Spencer, M.E., Huang, M.X., & Lewine, J.D. (1998) A study of dipole localization accuracy for MEG and EEG using a human skull phantom. *Electroencephalogr Clin Neurophysiol*, **107**, 159–173.

Legatt, A.D. & Kader, A. (2000) Topography of the initial cortical component of the median nerve somatosensory evoked potential. Relationship to central sulcus anatomy. *J Clin Neurophysiol*, **17**, 321–325.

Lemon, R.N. (1981) Functional properties of monkey motor cortex neurones receiving afferent input from the hand and fingers. *J Physiol*, **311**, 497–519.

Lin, Y.-Y., Shih, Y.-H., Chen, J.-T., Hsieh, J.-C., Yeh, T.-C., Liao, K.-K., Kao, C.-D., Lin, K.-P., Wu, Z.-A., & Ho, L.-T. (2003) Differential effects of stimulus intensity on peripheral and neuromagnetic cortical responses to median nerve stimulation. *Neuroimage*, **20**, 909–917.

Mauguiere, F. (2005) Somatosensory evoked potentials: normal responses, abnormal waveforms, and clinical applications in neurological disease. In *Electroencephalography. Basic Principles,*

Clinical Applications, and Related Fields, Niedermeyer E, Lopes da Silva F. edn. Lippincott, Williams & Wilkins, Philadelphia, pp. 1067–1119.

Mauguière, F., Merlet, I., Forss, N., Vanni, S., Jousmäki, V., Adeleine, P., & Hari, R. (1997) Activation of a distributed somatosensory cortical network in the human brain: a dipole modelling study of magnetic fields evoked by median nerve stimulation. Part II: effects of stimulus rate, attention and stimulus detection. *Electroencephalography and Clinical Neurophysiology/Evoked Potentials Section*, **104**, 290–295.

Mayhew, S.D., Mullinger, K.J., Bagshaw, A.P., Bowtell, R., & Francis, S.T. (2014) Investigating intrinsic connectivity networks using simultaneous BOLD and CBF measurements. *Neuroimage*, **99**, 111–121.

Mesulam, M.M. (1998) From sensation to cognition. *Brain*, **121 (Pt 6)**, 1013–1052.

Michel, C.M. & Brunet, D. (2019) EEG Source Imaging: A Practical Review of the Analysis Steps. *Front Neurol*, **10**, 325.

Michel, C.M. & He, B. (2019) EEG source localization. *Handb Clin Neurol*, **160**, 85–101.

Michel, C.M. & Murray, M.M. (2012) Towards the utilization of EEG as a brain imaging tool. *Neuroimage*, **61**, 371–385.

Michel, C.M., Murray, M.M., Lantz, G., Gonzalez, S., Spinelli, L., & Grave de Peralta, R. (2004) EEG source imaging. *Clin Neurophysiol*, **115**, 2195–2222.

Mideksa, K.G., Hellriegel, H., Hoogenboom, N., Krause, H., Schnitzler, A., Deuschl, G., Raethjen, J., Heute, U., & Muthuraman, M. (2012) Source analysis of median nerve stimulated somatosensory evoked potentials and fields using simultaneously measured EEG and MEG signals. *Conf Proc IEEE Eng Med Biol Soc*, **2012**, 4903–4906.

Morizot-Koutlidis, R., André-Obadia, N., Antoine, J.-C., Attarian, S., Ayache, S.S., Azabou, E., Benaderette, S., Camdessanché, J.-P., Cassereau, J., Convers, P., d'Anglejean, J., Delval, A., Durand, M.-C., Etard, O., Fayet, G., Fournier, E., Franques, J., Gavaret, M., Guehl, D., Guerit, J.-M., Krim, E., Kubis, N., Lacour, A., Lozeron, P., Mauguière, F., Merle, P.-E., Mesrati, F., Mutschler, V., Nicolas, G., Nordine, T., Pautot, V., Péréon, Y., Petiot, P., Pouget, J., Praline, J., Salhi, H., Trébuchon, A., Tyvaert, L., Vial, C., Zola, J.-M., Zyss, J., & Lefaucheur, J.-P. (2015) Somatosensory evoked potentials in the assessment of peripheral neuropathies: Commented results of a survey among French-speaking practitioners and recommendations for practice. *Neurophysiol Clin*, **45**, 131–142.

Mouchnino, L., Lhomond, O., Morant, C., & Chavet, P. (2017) Plantar Sole Unweighting Alters the Sensory Transmission to the Cortical Areas. *Front Hum Neurosci*, **11**, 220.

Nachev, P., Kennard, C., & Husain, M. (2008) Functional role of the supplementary and pre-supplementary motor areas. *Nat Rev Neurosci*, **9**, 856–869.

Nakamura, A., Yamada, T., Goto, A., Kato, T., Ito, K., Abe, Y., Kachi, T., & Kakigi, R. (1998) Somatosensory homunculus as drawn by MEG. *Neuroimage*, **7**, 377–386.

Oldfield, R.C. (1971) The assessment and analysis of handedness: the Edinburgh inventory. *Neuropsychologia*, **9**, 97–113.

Onishi, H., Sugawara, K., Yamashiro, K., Sato, D., Suzuki, M., Kirimoto, H., Tamaki, H., Murakami, H., & Kameyama, S. (2013) Effect of the number of pins and inter-pin distance on somatosensory evoked magnetic fields following mechanical tactile stimulation. *Brain Res*, **1535**, 78–88.

Papadelis, C., Eickhoff, S.B., Zilles, K., & Ioannides, A.A. (2011) BA3b and BA1 activate in a serial fashion after median nerve stimulation: direct evidence from combining source analysis of evoked fields and cytoarchitectonic probabilistic maps. *Neuroimage*, **54**, 60–73.

Passmore, S.R., Murphy, B., & Lee, T.D. (2014) The origin, and application of somatosensory evoked potentials as a neurophysiological technique to investigate neuroplasticity. *J Can Chiropr Assoc*, **58**, 170–183.

Peterson, N.N., Schroeder, C.E., & Arezzo, J.C. (1995) Neural generators of early cortical somatosensory evoked potentials in the awake monkey. *Electroencephalogr Clin Neurophysiol*, **96**, 248–260.

Pierrot-Deseilligny, E. & Burke, D. (2005) *The Circuitry of the Human Spinal Cord*. Cambridge

916   University Press, New York, USA.

917   Porcaro, C., Coppola, G., Pierelli, F., Seri, S., Di Lorenzo, G., Tomasevic, L., Salustri, C., & Tecchio, F.
918   (2013) Multiple frequency functional connectivity in the hand somatosensory network: an EEG
919   study. *Clin Neurophysiol*, **124**, 1216–1224.

920   Pratt, H., Politoske, D., & Starr, A. (1980) Mechanically and electrically evoked somatosensory
921   potentials in humans: effects of stimulus presentation rate. *Electroencephalogr Clin*
922   *Neurophysiol*, **49**, 240–249.

923   Rezaei, A., Lahtinen, J., Neugebauer, F., Antonakakis, M., Piastra, M.C., Koulouri, A., Wolters, C.H., &
924   Pursiainen, S. (2021) Reconstructing subcortical and cortical somatosensory activity via the
925   RAMUS inverse source analysis technique using median nerve SEP data. *Neuroimage*, **245**,
926   118726.

927   Rizzolatti, G. & Craighero, L. (2004) The mirror-neuron system. *Annu Rev Neurosci*, **27**, 169–192.

928   Sakura, Y., Terada, K., Usui, K., Baba, K., Usui, N., Umeoka, S., Yamaguchi, M., Matsuda, K., Tottori, T.,
929   Mihara, T., Nakamura, F., & Inoue, Y. (2009) Very high-frequency oscillations (over 1000 Hz) of
930   somatosensory-evoked potentials directly recorded from the human brain. *J Clin Neurophysiol*,
931   **26**, 414–421.

932   Sangari, S., Iglesias, C., El Mendili, M.-M., Benali, H., Pradat, P.-F., & Marchand-Pauvert, V. (2016)
933   Impairment of sensory-motor integration at spinal level in amyotrophic lateral sclerosis. *Clin*
934   *Neurophysiol*, **127**, 1968–1977.

935   Saradjian, A.H., Tremblay, L., Perrier, J., Blouin, J., & Mouchnino, L. (2013) Cortical facilitation of
936   proprioceptive inputs related to gravitational balance constraints during step preparation. *J*
937   *Neurophysiol*, **110**, 397–407.

938   Schabrun, S.M., Ridding, M.C., Galea, M.P., Hodges, P.W., & Chipchase, L.S. (2012) Primary sensory
939   and motor cortex excitability are co-modulated in response to peripheral electrical nerve
940   stimulation. *PLoS ONE*, **7**, e51298.

941   Schoffelen, J. & Gross, J. (2009) Source connectivity analysis with MEG and EEG. *Hum Brain Mapp*, **30**,
942   1857–1865.

943   Solopchuk, O., Alamia, A., & Zénon, A. (2016) The Role of the Dorsal Premotor Cortex in Skilled Action
944   Sequences. *J Neurosci*, **36**, 6599–6601.

945   Tadel, F., Baillet, S., Mosher, J.C., Pantazis, D., & Leahy, R.M. (2011) Brainstorm: A User-Friendly
946   Application for MEG/EEG Analysis. *Computational Intelligence and Neuroscience*, **2011**, 1–13.

947   Tadel, F., Bock, E., Niso, G., Mosher, J.C., Cousineau, M., Pantazis, D., Leahy, R.M., & Baillet, S. (2019)
948   MEG/EEG Group Analysis With Brainstorm. *Front Neurosci*, **13**, 76.

949   Tanji, J. & Wise, S. (1981) Submodality distribution in sensorimotor cortex of the unanesthetized
950   monkey [WWW Document]. *Journal of neurophysiology*,. URL
951   https://pubmed.ncbi.nlm.nih.gov/7218010/

952   Tecchio, F., Zappasodi, F., Pasqualetti, P., & Rossini, P.M. (2005) Neural connectivity in hand
953   sensorimotor brain areas: an evaluation by evoked field morphology. *Hum Brain Mapp*, **24**, 99–
954   108.

955   Torquati, K., Pizzella, V., Della Penna, S., Franciotti, R., Babiloni, C., Rossini, P.M., & Romani, G.L.
956   (2002) Comparison between SI and SII responses as a function of stimulus intensity.
957   *Neuroreport*, **13**, 813–819.

958   Tumati, S., Martens, S., de Jong, B.M., & Aleman, A. (2019) Lateral parietal cortex in the generation of
959   behavior: Implications for apathy. *Prog Neurobiol*, **175**, 20–34.

960   Urasaki, E., Genmoto, T., Akamatsu, N., Wada, S., & Yokota, A. (2002) The effects of stimulus rates on
961   high frequency oscillations of median nerve somatosensory-evoked potentials--direct
962   recording study from the human cerebral cortex. *Clin Neurophysiol*, **113**, 1794–1797.

963   Valeriani, M., Le Pera, D., & Tonali, P. (2001) Characterizing somatosensory evoked potential sources
964   with dipole models: advantages and limitations. *Muscle Nerve*, **24**, 325–339.

965   **TABLES**

Hemisphere	areas	P20/N20		P60/N60		P100/N100	
		MEG	EEG	MEG	EEG	MEG	EEG
Contralateral	SI						
	SII						
	M1						
	SMA						
	PM						
	sPPC						
	iPPC						
	SMG						
	PCC						
	STS						
	Insula						
Ipsilateral	SI						
	SII						
	M1						
	SMA						
	PM						
	sPPC						
	iPPC						
	SMG						
	PCC						
	STS						
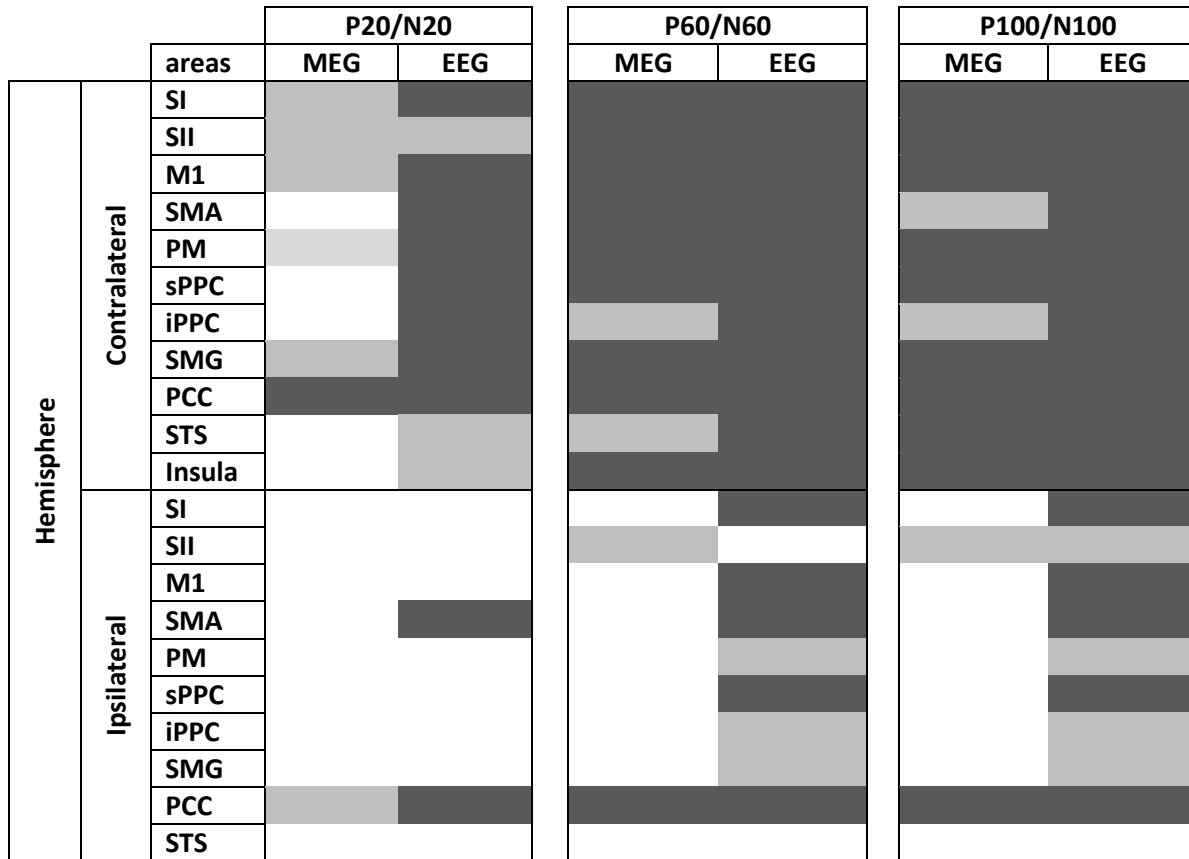
966 **Table 1. Reliability of significant source activity.** Proportion of subjects with significant source

967 activity (according to Z-score threshold after Bonferroni correction for multiple comparison) during

968 P20/N20, P60/N60 and P100/N100 in MEG and EEG at the level of the ROIs on both contra- and

969 ipsilateral hemispheres. Dark grey when more than 75 % of the participants exhibited significant Z-

970 score, light grey, between 50 and 75% and white when less than 50 %.

		1.5 x PT	3 x PT	6 x PT	9 x PT
MEG	P20/N20 vs. P60/N60	0.025	0.0152	< 0.0001	< 0.0001
	P20/N20 vs. P100/N100	0.8740	0.0871	< 0.0001	< 0.0001
	P60/N60 vs. P100/N100	0.0167	0.4608	0.5298	0.4714
EEG	P20/N20 vs. P60/N60	< 0.0001	< 0.0001	< 0.0001	< 0.0001
	P20/N20 vs. P100/N100	0.099	< 0.0001	< 0.0001	< 0.0001
	P60/N60 vs. P100/N100	0.0171	0.6464	0.0353	0.3702

971 **Table 2. *Post hoc* comparisons of components according to the intensity**. *P*-values of *post*

972 *hoc* Student's t-tests comparing Z-score least-squares means between components

973   according to the intensity of median nerve stimulation. Squares in grey indicate non-

974   significant differences.

975   **FIGURE LEGENDS**

976   **Figure 1: Raw MEG and EEG epochs in one individual. AB**, Superimposition of the mean epochs (n =

977   600 stimuli) at the level of each MEG (**A**) and EEG (**B**) sensor, around median nerve stimulation

978   adjusted at 6xPT. **CD**, mean epochs at the level of each sensor over the brain cortex in MEG (**C**) and

979   EEG (**D**). **EF**, topography of the mean MEG (**E**) and EEG (**F**) activity, according to the corresponding

980   gradient of colours, 20 ms (left figurine), 60 ms (middle figurine) and 85 ms (right figurine) after

981   median stimulation (indicated in **AB** by vertical red arrows).

982   **Figure 2: Mean normalised MEG and EEG source activity in the brain cortex during early and late**

983   **SEPs. AB**, Time course of mean normalised current in each individual (black lines) and their grand

984   average around median nerve stimulation adjusted at 6 x PT (red line; between -20 ms and 120 ms):

985   the Z-scores of current densities were extracted after MEG (**A**) and EEG (**B**) source analysis, at the

986   level of the post-central cortex corresponding to the primary somatosensory area (SI). Each black

987   trace corresponds to the results of 1 participant and the red line results from the grand average of

988   the 19 participants. **CH**, normalised source activity from MEG (**CE**) and EEG (**FH**) in the group of

989   participants (n = 19) with, in each figurine, upper left, the left hemisphere, lower left, le right

990   hemisphere, and on the right, the top view of the brain. The Z-score of mean current density was

991   extracted for each window of analysis corresponding to P20/N20 (**C,F**), P60/N60 (**D,G**) and

992   P100/N100 (**E,H**) in each individual and projected into the common MNI space. The gradient of

993   colours corresponds to Z-scores from 0 (dark blue) to 20 (dark red), with a threshold estimated at Z-

994   score = 4.02 after *p*-value correction (Bonferroni correction for multiple comparisons; thin line within

995   the blue area in the legend). Accordingly, only significant activity (*p*-value < 0.000058) are illustrated

996   (> 20 % of the maximum amplitude of the gradient).

997   **Figure 3: Hierarchy of activated brain areas in the group**. The ROIs are organised according to the

998   proportion of subjects in the group (n = 19) with MEG (**A**) and EEG (**B**) activity after median nerve

999   stimulation (6 x PT) significantly different from baseline (Z-score ≥ 4.02, *p*-value < 0.000058). Each

1000   level of the hierarchy is represented by one ring and the larger the part of the ring per item, the

1001   greater the proportion of subjects with significant Z-score. The first level of hierarchy includes the

1002   ROIs in the contralateral (c.) and ipsilateral (i.) hemispheres. The second level includes the 3

1003   components. The proportions ≥ 50 % are indicated in white and those ≥ 75%, in red.

1004   **Figure 4: Relationship between stimulus intensity and normalised source activity in early and late**

1005   **SEPs.** The Z-scores of mean current density (n = 19 participants) in MEG (**A,C,E**) and EEG (**B,D,F**), in

1006   the 3 windows of analysis corresponding to P20/N20 (**AB**), P60/N60 (**CD**) and P100/N100 (**EF**) for the

1007   main areas activated, are plotted against the intensity of the median nerve stimulation, normalised

1008   to the perceptual threshold (x PT). Interrupted lines indicate the threshold for significant Z-score (≥

1009   4.02, according to Bonferroni correction for multiple comparisons). Vertical bars are ± 1 SD.

1010   **Figure 5: Prediction of MEG and EEG early and late components according to the stimulus intensity**.

1011   Z-score least-squares means from the repeated-measures linear mixed-effects model are plotted

1012   against the intensity of median nerve stimulation (normalised to the perceptual threshold, xPT; **A,CD**)

1013   or the SEP components (**B**) extracted from MEG (red dots and lines in **AB**) and EEG source analysis

1014   (black dots and lines in **AB**), at the latency of P20/N20 (blue dots and lines in **CD**), P60/N60 (red dots

1015   and lines in **CD**) and P100/N100 (green dots and lines in **CD**) from MEG (**C**) and EEG (**D**). Vertical bars

1016   are ± 1 SD. *** *p*-value < 0.001, ** *p*-value < 0.01 after *post hoc* comparisons of two means

1017   (Student's t-tests on least-square means; in **AB**). *P*-values for **CD** are indicated in Table 2.

1018   **Figure 6: Prediction of the influence of stimulus intensity in ROIs**. Z-score least-squares means from

1019   the repeated-measures linear mixed-effects model calculated at 1.5 (light grey dots and lines), 3

1020   (middle grey dots and lines), 6 (dark grey dots and lines) and 9 x PT (black dots and lines) are plotted

1021   against the regions of interests (ROIs) for MEG (**A**) and EEG (**B**). Vertical bars are ± 1 SD.

1022 **Figure 7: Prediction of early and late components in ROIs**. Z-score least-squares means from the

1023 repeated-measures linear mixed-effects model calculated at the latency of P20/N20 (blue dots and

1024 lines), P60/N60 (red dots and lines) and P100/N100 (green dots and lines) for MEG (**A**) and EEG (**B**).

1025 Vertical bars are ± 1 SD.

1026 **AUTHOR CONTRIBUTION**

1027 VMP, NG and DS conceptualised the study and has developed the protocol. SHK, CG and VMP

1028 performed the experiments. SHK and VMP performed the analysis under the supervision of CH, NG

1029 and DS. GM and MLVQ have supervised and validated the methodology. VMP and AG have

1030 performed the statistical analysis. SHK has drafted the manuscript which was fully revised by VMP

1031 and GM. All authors participated in finalising the manuscript.

1032 **CONFLICT OF INTEREST**

1033 None of the authors have potential conflicts of interest to be disclosed.

1034 **GRAPHICAL ABSTRACT TEXT**

1035 - Early and late components exhibit distinct features and are not correlated.

1036 - Late responses are not characteristic of SII area only but include more complex cortico-cortical

1037 neural networks.

1038 - Besides some overlapped activity in early and late responses, distinct networks participate in
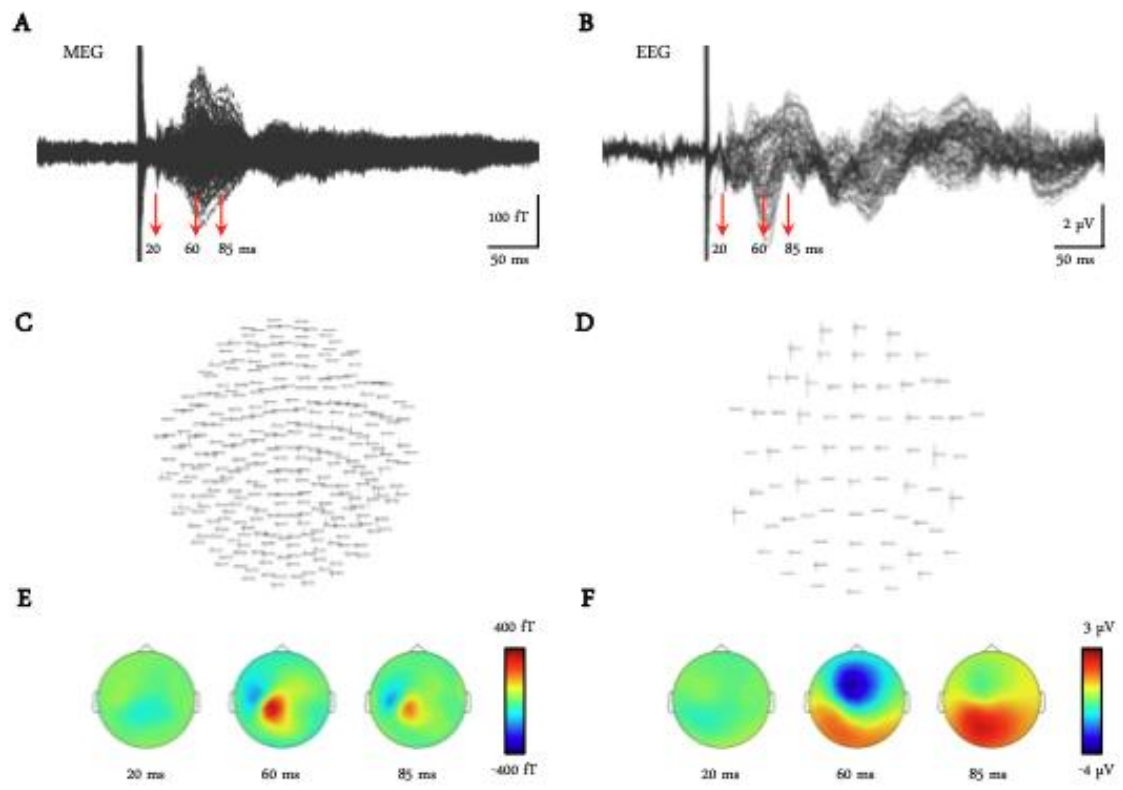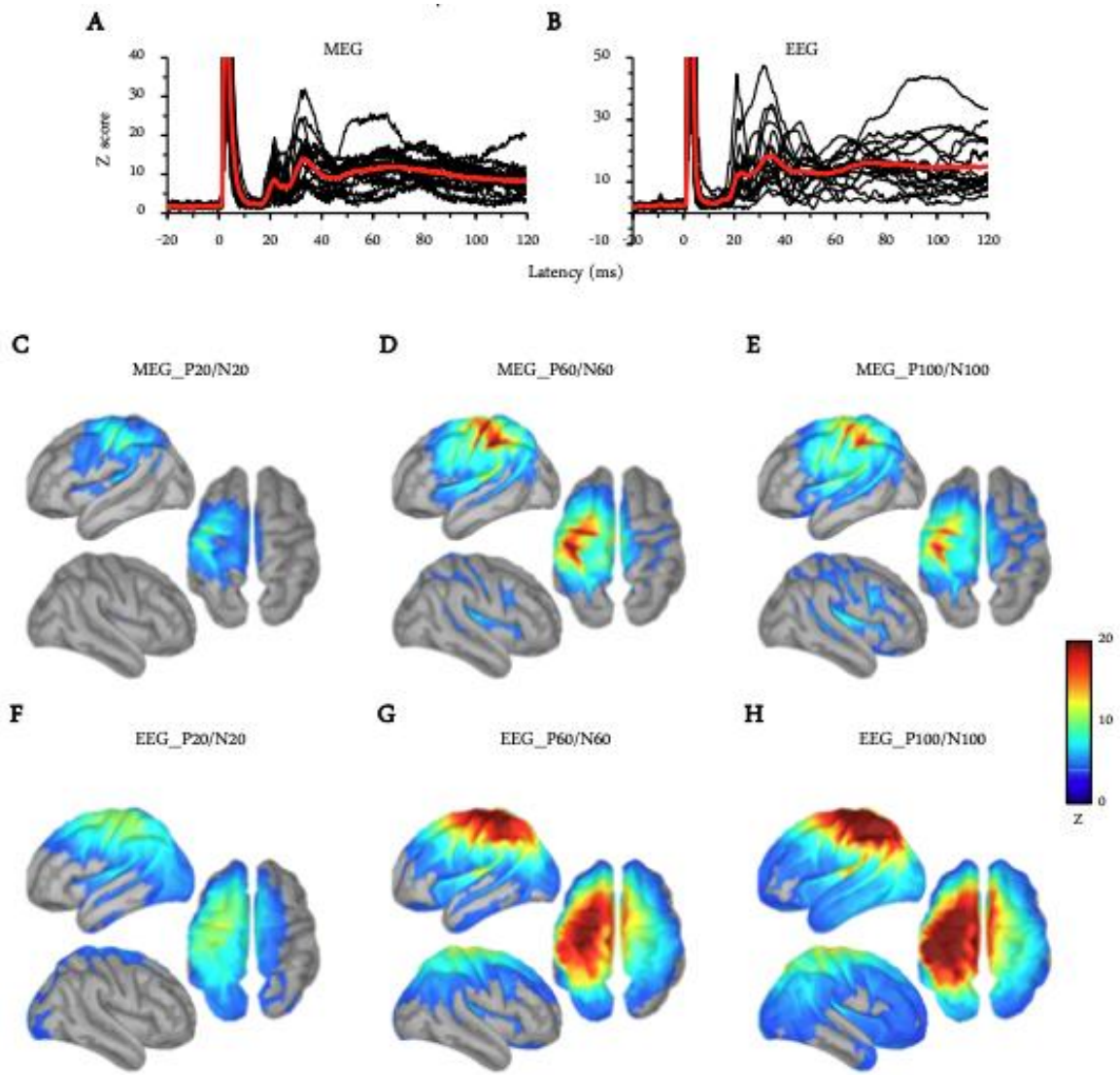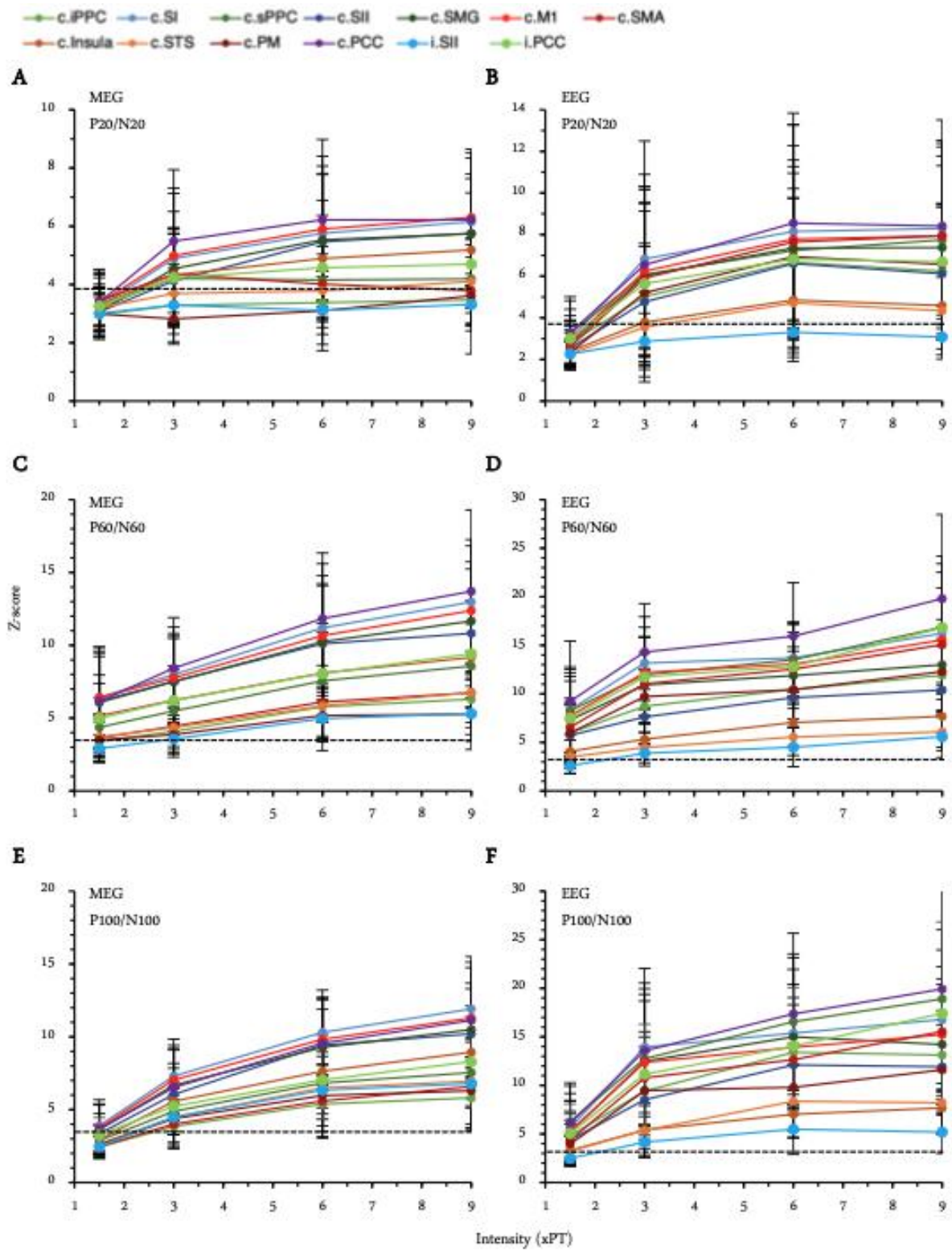
1039 somatosensory brain processing.

1040

A — MEG
B — EEG
C
D
E

20 ms   60 ms   85 ms

F

20 ms   60 ms   85 ms

Figure 2

1043

1044

39

A

B

MEG

EEG

- c.SI
- c.SII
- c.sPPC
- c.iPPC
- c.SMG
- c.PCC
- c.M1
- c.PM
- c.SMA
- c.STS
- c.Insula
- i.iPPC
- i.M1
- i.PCC
- i.PM
- i.SI
- i.SII
- i.SMA
- i.sPPC
- i.STS

Figure 3

Legend: c.iPPC, c.SI, c.sPPC, c.SII, c.SMG, c.M1, c.SMA, c.Insula, c.STS, c.PM, c.PCC, i.SII, i.PCC

A MEG P20/N20
B EEG P20/N20
C MEG P60/N60
D EEG P60/N60
E MEG P100/N100
F EEG P100/N100

Z-score

Intensity (xPT)

1047

1048

Figure 4

A

MEG

B

EEG

1051

Figure 6

44